Accepted Manuscript

Mechanical behaviors and failure mechanisms of Buried Polyethylene pipes crossing active strike-slip faults

Jie Zhang, Yao Xiao, Zheng Liang

PII: S1359-8368(18)30978-8

DOI: 10.1016/j.compositesb.2018.09.006

Reference: JCOMB 5976

To appear in: *Composites Part B*

Received Date: 26 March 2018

Revised Date: 15 August 2018

Accepted Date: 4 September 2018

Mechanical Behaviors and Failure Mechanisms of Buried Polyethylene Pipes Crossing Active Strike-slip Faults

Jie Zhang*, Yao Xiao, Zheng Liang

School of Mechatronic Engineering, Southwest Petroleum University, Chengdu, 610500, China

*Correspondence author: J. Zhang, E-mail: longmenshao@163.com

Abstract: Polyethylene (PE) pipes are widely used in gas transmission projects due to their excellent performances. Earthquake is destructive and difficult to predicted, which is one of the major disasters caused PE pipe failure. The study was conducted on the mechanical behaviors and failure mechanisms of buried PE pipes under fault movement, and the effects of gas pressure, fault dislocation, soil and pipe size on the mechanical behavior of PE pipes were discussed. The study indicates that gas pressure has a less effect on the mechanical behavior of PE pipe. Under faults, the flatness curve of PE pipe is distributed symmetrically with respect to the fault plane. Deformation rules of PE pipe in different stratums are similar, while the pipe deformation is the largest in clay and it is smallest in sand. The greater the standard pipe size, the greater the diameter flatness coefficient is. The larger the diameter, the smaller the pipe diameter flattening parameter is. PE pipes with a larger the standard dimension ratio of a fitting (*SDR*) and a smaller diameter are prone to failure in fault zone. The results can provide the basis for gas pipe design, laying, testing, and evaluation.

Key words： Polyethylene pipe; Strike-slip fault; numerical simulation; mechanical behavior; Failure analysis

1 Introduction

In recent years, the demand for energy has increased[1]. Urban gas pipes, hailed as the city's lifeline, have a crucial role to play in sustaining urban functions. Common gas pipes are made from the steel pipe, cast iron, PE pipe and other components. Steel pipe and cast iron pipe are gradually replaced by PE pipe in the gas pipe projects due to its flexibility, corrosion resistance, weldability and other characteristics[2-4]. "Steel-to-plastics substitution" has become mainstream in the pipe field [5]. In the rapid development of PE gas pipe, the concern of its safe operation is also increasing rapidly. So far, the safe operation of gas with PE pipe will be directly affected by the external damage, repair mistakes, pipe corrosion, material failure, geological disasters and other reasons[6]. Among them, stratum permanent deformation caused by unpredictable and sudden geological disasters serves as one of the main causes of the buried pipe failure. Pipe failure may cause serious accidents, such as explosion and fire [7]. Therefore, it is necessary to study the mechanics behavior and failure mechanism of buried PE pipe under earthquake fault.

For current researches, the study on the mechanical system of buried steel pipes with complex situation goes well, but PE pipes not. An evaluation methodology mixed with fault tree analysis (FTA), analytic hierarchy process (AHP) and the grey theory is applied to the risk assessment of urban PE gas pipes by Guo et al.[8]. Based on the Kent scoring method, Jin et al.[5] have established the risk factor evaluation system of PE gas pipe with a more optimizing semi-quantitative method. A system for medium pressure PE pipes was established by Liang [7]. The system with hierarchical-expert consultation comprehensive evaluation method determined the weight of each risk evaluation criteria, managed the risk value and some targeted measures could be taken to improve the safety and reliability of the pipe. Zhou [6] have analyzed the deformation damage of PE pipes within soil settlement and collapse situations through experimental simulations. The deformation characteristics and failure laws of PE pipes with different diameter, wall thickness and depth are analyzed. Aimed at the failure influence factor of the buried PE gas pipes under traffic load, a mechanical analysis method was set up on the actual engineering by Li [3]. Meanwhile, a simple experiment was designed to test the mechanical properties of PE pipes and provided a reference for the safety evaluation and mechanical properties test combined with mechanics. Guo [9] established the finite element model of buried PE pipe with traffic loads, analyzed pipe failure and proposed some countermeasures policies for self-safety, safety-distance and safety-management. Based on Suleiman hyperbolic model, Ma et al. [10,11] confirmed the failure criteria through the yield failure criteria of PE pipes from the tensile experiments. Moghaddas and Khalaj [12] studied the mechanical performance of buried PE pipes with traffic loads by simulation. By analyzing the radial deformation , and separately discussions and the influence of different soil and buried depth on the deformation and settlement were carried out .

Mechanical behaviors and failure mechanisms of cross-fault buried PE pipes under the earthquake fault were investigated in this paper. Pipe-soil system was analyzed nonlinearly to determine the failure criteria of the PE pipe. The typical parameters were selected to study the effect of different fault dislocations and soils on the strength of non-pressure and pressure PE pipes respectively. At the same time, the deformation rules of PE pipes with different sizes after being squeezed by the fault were analyzed. The failure mechanism of buried PE gas pipe under cross-fault motion was studied, which had a certain value for the development of risk assessment system of post-geological gas pipe.

2 Mechanical response of buried PE pipes

2.1 Nonlinear finite element

（1） PE pipe

As a polymer, polyethylene has the property of viscoelasticity. Its mechanical properties are affected by four factors, such as force, deformation, temperature and time[3]. The strain rate sensitivity is more obviously than that of metal material. The use of polymeric composites has grown at a phenomenal rate, and these materials now have impressive and diverse range of applications[13].

Suleiman [14] and others proposed hyperbolic constitutive mode as follows：

$$\sigma = \frac{\varepsilon}{a + b\varepsilon} \tag{1}$$

Among them, the parameters a and *b* are related to the tensile-strain rate. σ and ε are real stress and strain. Then, the initial modulus of the PE pipe can be obtained:

$$E_i = \frac{1}{a} \tag{2}$$

The Eq.(1) is linearly converted:

$$\frac{\varepsilon}{\sigma} = a + b\varepsilon \tag{3}$$

According to the stress-strain data of the uniaxial tension in the test[11], when Eq.(3) is calculated, the values of parameters *a* and *b* can be fitted. The fitted constitutive relationship is in good agreement with the experimental data, and it is able to accurately simplify and simulate the material properties of polyethylene material (PE80)[15]. For nonlinear materials, magnetic nanoparticle has some advantages, such as high stability, strong magnetic responsiveness, cost effectiveness and excellent binding of a larger value of lysozyme and easier separation from the reaction system[16]. Nanomaterials have attracted extensive attention because of their novel properties in different fields in comparison with their bulk counterparts[17]. And enzymes are natural biocatalysts of nanometer scale[18]. About thermal stability of nanocomposites, which was characterized by X-ray diffraction, scanning electron microscopy and so on[19]. Development of nanocatalysts for hydrogen sorption with high performance and stout stability remained as one of the most important challenges for energy conversion/storage[20].

The material of PE pipes is viscoelastic and isotropic. The constitutive model of PE pipe with the strain rate is $2.5s^{-1}$was analyzed, the performance parameters as shown in Table 1 and Fig.1.

（2） Soil model

The commonly used soil models are the Mohr-Coulomb (M-C) and the Drucker-Prager (D-P). In this paper, the plastic model of Mohr-Coulomb (M-C) is used, which is suitable for materials with grain characteristics under monotonic loading. The general criterion equation, as follows:

$$\tau_n = f\left(c, \varphi, \sigma_n\right) \tag{4}$$

Where, c is the cohesive force of soil. φ is the internal friction angle of the soil. σ_n is the positive stress on the yield surface.

M-C model is suitable for sensitive soils, which is a good reflection of the behavior of rocks and soils under tensile and compressive loads, widely used. Moreover, the M-C model ignores the influence of the intermediate principal stress and the hydrostatic pressure, and the results calculated by are more conservative this model[21]. The length and width of the model are large enough to simulate infinite soil. The property is shown as Table 2.

（3） Pipe-soil system

The interaction is finite-slip contact between pipe and soil. Coulomb friction model is used to define the tangential motion, and the friction coefficient to represent the friction characteristics between the contact surfaces[22]. According to different friction behaviors between PE pipe and several soils, and friction coefficient in the range of 0.45~0.7[23]. Moore Coulomb's calculation formula is:

$$\tau_{crit} = \mu \times p \tag{5}$$

Where, τ_{crit} is the critical shear stress, μ is the friction coefficient, and p is the normal contact pressure. Before the tangent force increases to the critical shear stress, there will be no relative sliding between the friction surfaces.

2.2 PE pipe performance criteria

There are two failure modes of the PE pipe under inner pressure: ductile failure and brittle failure. The ductile failure is the creep expansion of the PE pipe under the high inner pressure. That is to say, the weakest point of the pipe suddenly bumps up and destroy quickly at a certain time. The brittle failure is the damage caused by the small crack growth under the smaller inner pressure. In addition, there may be third types of damage to the PE pipe aging resulting in brittle failure, which usually occurs after 50 years. The sketch map of the PE pipe failure mode is shown in Fig.2.

The hydrostatic strength of both failure modes is a decreasing function of time. Compared with ductile failure, hydrostatic strength of brittle failure decreased more steeply. With the increasing of the PE pipe's service time, the failure mode will change from ductile failure to brittle failure under constant pressure, namely the toughness-brittleness transition[24], as shown in Fig.2. At present, the research on the failure mode of pipe mainly relies on the experiment to complete [3].

(1) Strength failure criterion

Due to the unique viscoelasticity of PE pipe and the failure mode is plastic failure under a large load and short time, it is infeasible to use the fourth strength theory as the failure criterion of PE pipe[25].

Referring to "*Buried Polyethylene (PE) Pipeline System for Gas*" [14], the minimum required strength of PE pipes is chosen as the strength failure criterion of the pipe. The common types of gas pipes are PE80 and PE100. The minimum required strength of PE80 is 8.0MPa, and that of PE100 is 10.0MPa.

(2) Strain failure criterion

Under the external load, the strain establish the local relative deformation of the PE pipe. For the PE pipe, it suggested that the strain control within 5%[26]. Therefore, the strain limit is 5%.

(3) Deformation failure criterion

The material deformation is divided into elastic deformation and plastic deformation. Elastic deformation is able to restore the original shape after the withdrawal of external force. Plastic deformation is unable to restore the original shape after the withdrawal of external force, the shape of elongation or shortening[27].

For pipes with many materials, the maximum design allowable deformation is 5%. However, about the flexible PE pipe with a high resistance to deformation ability, the deformation of 5% is relatively conservative, and its short-term deformation limit is able to reach 30%[28]. However, it is generally considered that the pipe will not be damaged when the deformation of PE pipe reaches 20%[29]. When the safety coefficient of PE pipe is 1.5, the deformation limit of PE pipe is 20%.

For safe operation of the pipe, significant cross-section distorition should be avoided. The strike-slip fault movement causes local bending and flattening or ovalization of the pipe cross-section, and that can be expressed through the non-dimension "flattening parameter" f [24], defined as follows :

$$f = \frac{\Delta D}{D} \tag{6}$$

$\Delta D=D_V-D$ or $\Delta D=D_H-D$, where ΔD is the maximum change of diameter. A cross-sectional flattening (serviceability) limit state is assumed when the value of f becomes equal to 20%**.**

3 Numerical modeling

Finite element analysis (FEA) is a mathematical approximation method to simulate real physical systems, including geometry and load，by simplifying complex problems[26]. Therefore, the structural response of buried PE80 pipes under strike-slip fault movement is examined numerically using more advanced finite element analysis tools. 3D model of the buried PE pipes crossing strike slip faults is established considering the pipe-soil coupling. For the limit of wall thickness of the shell model, solid models are used for the pipe and soil. So the simulation model is closer to the engineering practice.

As shown in Fig. 3, the boundary conditions and contact are illustrated reasonably. About interaction: **a.** and **b.** are soil-pipe: moving contact method (surface and surface contact); **c**. is fault-pipe: self-contact of surface; fault-soil: tangential behavior (penalty function), friction coefficient is 0.5. About load: restrict movement of Y and Z direction on both sides of soil bottom. The right and left sides move uniformly on the X direction, and the amplitude function is shown in the figure. In kinematic modeling of fault dislocation, the dislocation can be imposed by displacement vectors on the two sides of the fault plane. Because of the nonlinear static analysis, the fault free dislocation function can be a uniformly varying fault, as shown in Fig.4.

As shown in Fig.5, dividing the pipe and soil solids into hexahedron eight-node (C3D8R) unit, respectively. The mesh of pipe and soil part are refined in the area of dislocation. PE80 has a better disturbability, and it is easy to roll, flattening resistance, and widely used in small and medium caliber. PE100 is used in large diameter pipes. According to the requirements: the minimum covering thickness of the underground gas pipe laid under the driveway is not less than 0.9m, and the place where the vehicle can't arrive is not less than 0.5m. This paper selects PE80 medium density polyethylene gas pipe (MDPE), the analytical pipe segment is 20m, the buried depth is 0.5m, the Standard dimension ratio of a fitting (*SDR*) is 11, outer diameter (*D*) is 110mm, and thickness (*t*) is 10mm. The gravity g is 9.8m/s^2. The effects of internal pressure on pressurized and non-pressurized pipes are simulated, respectively. PE gas pipe's *SDR*=11 with the maximum operating inner pressure (P_{max}) to 0.8MPa, and the pipe's *SDR*=17.6 with the P_{max} to 0.4MPa.

The rationality of the model is verified as shown in Fig. 6. It can be clearly seen from the simulation results that the length of the pipe affected by faults is much less than 20m, so the length of the model set in this paper is sufficient. In order to study the sufficiency of cross-sectional dimension, the contact model of slip fault pipe-soil is set up. The specific size difference between Model 1 and Model 2 is shown in the figure. In order to ensure the comparability of the results, keep the buried depth of PE pipe unchanged and increase the thickness of soil under the pipe, the model size was changed to 4×2×20m, and the pipe displacement was analyzed after the same slip fault. By comparing the results of two groups of models with different sizes, it can be seen that there is little difference between the two groups of curves. The finite analysis results of the two sets of models for simulating actual faults are almost the same. Therefore, the size of the model established in this paper is suitable and the acceptable results are obtained.

In order to study the rationality of the slip fault angle, we have done some related research as shown in Fig.7. Comparative analysis and evaluation of different inclination angles was added. 90 degree，60 degree and 45 degree dip fault zones are named Model 3, Model 4 and Model 5, respectively. The same dislocation was used to analyze the difference of mechanical response of three groups of dip fault motion to PE pipe in soil. The displacement curve of PE pipe in the direction of fault is extracted when the dislocation is 2*D*. From the displacement curves, we can see that the displacement trends of the three angles are similar, so the change of the angle has little effect on the qualitative research, and both sides of the fault plane are symmetrical. But it can be clearly seen that the three groups of strike-slip fault dip angle will affect the soil PE pipe displacement variation of the extreme value is different. When the inclination angle is 90 degree, the displacement variation of the pipe is larger than that of the other two groups, and the deformation is more serious, so the pipe is more dangerous. In order to analyze the damage degree of the fault to the pipe to a greater extent, we choose 90 degree inclination angle which will lead to the maximum deformation displacement of the pipe, and the inclination angle has no influence on the change trend research.

In order to avoid the influence of the number of grids on the analysis results, we made a comparative analysis, as shown in the Fig.8. Three sets of finite element models with different mesh number were set up for analysis, and curves of displacement fields under a certain dislocation were shown in the figure. The number of grids in Mesh 1, Mesh 2 and Mesh 3 increases in sequence. In this paper, three groups of models with different mesh densities are simulated and analyzed, and displacement field curves caused by dislocation of the same slip fault are extracted. It is clearly found that the Mesh 1 model with the smallest mesh number has slight extremum difference with the other two models, and the influence range of fault behavior is smaller and the change is faster. However, the difference between Mesh 2 and Mesh 3 is very small, and the curves coincide basically, so the effect of increasing the mesh number on the results is very small. Considering the larger number of grids, the analysis takes longer. Therefore, it is necessary to select the appropriate number of grids to ensure the accuracy of the results, so we choose Mesh 2 as the grid generation standard.

The comparison of clay, silty clay, loess and sand in four kinds of soil materials. The soil block has dimensions 2m×1m×20m, in which an almost rigid D = 0.11m pipe is buried.

4 Results and discussions

4.1 Mechanical behavior of non-pressure pipe

4.1.1 Effect of fault displacement

Fig.9 shows deformation of the pipe-soil system under the strike-slip fault. Before the fault, the surrounding cohesive soils are completely contacted to the the pipe surface. The PE pipe bears the pressure of the soil and the gravity. With the movement of soil, buried pipe is bent out of shape in the soil, but the deformation section still maintains a smooth curve. PE pipe and soil separation occurs locally. One side of pipe segment is separated from the soil, and the fault causes the buried PE pipe to withstand the friction of the surrounding soil. However, the other side of the pipe is closer to the other side of the soil. Because the soil is soft and easy to deform, the deformation of the pipe also affects the deformation of the surrounding soil.

Fig.10 shows the pipe-soil system in the process of fault in the X-axis direction. It shows von Mises stresses of the separated pipe segment and soil in the fault zone. The stress varies greatly on the contact surface of the pipe and soil on both sides of the fault. In particular, it is increasing rapidly the compression and tensile side during deformation part. Small gap occurs at the soil -pipe interface under fault. In the process of fault movement, the soil pressure on the pipe is different, which leads to the friction of the whole pipe segment is not homogeneity. Therefore, it is very important to take the appropriate friction coefficient of pipe and soil.

Separated the affected pipe segment from the pipe-soil system, the non-pressure pipe is mainly subjected to axial tensile stress, and the stress on the principal stress surface is maximum. Therefore, the principal stress as a reference to analyze the force of the pipe. Fig.11 shows principal stress under different fault displacements, and the high-low stress distribution are obvious and regular. The high stress area is concentrated around the contact surface of the pipe-soil near the fault layer for the PE pipe is subject to bending moment under the fault movement. In the bend part of the pipe, the stress concentration occurs at the location with a the minimum curvature. With the gradual increasing of the fault displacement, the high stress zone of PE pipe is slightly extended from the center of the fault and expands evenly, showing the symmetry of the two sides. Because the physical properties of polyethylene material different from metal material, PE pipe shows a smooth curve in the area of bending deformation without local energy accumulation in the process of increasing the fault momentum from 0 to 4*D*. Therefore, there was no local crushing to result in the damage of PE pipe.

Fig.12 shows axial stress curves of PE pipe in different displacements. The amount of dislocation has a great influence on the axial stress around the fault area. PE pipe’s axial stress curve is center symmetry, and presents the shape of "S". With the increasing of fault dislocation, the deformed pipe is larger, the greater the range of "S". Obviously, the axial stress is 0 in the far away from the fault plane 1.5m outside. In other words, apart from a distance from a fault, the pipe is almost unaffected by the fault.

Fig.13 shows the curves of the maximum axial stress and the maximum principal stress with the fault dislocations. The two curves are the same trend. The maximum principal stress is higher than the maximum axial stress, but the difference between the two sets of data is very small. Notably, PE pipe is mainly affected by the axial stress in the fault. It is feasible to use the main stress to analyze the mechanical behavior of PE pipe. In the first stage (0.5*D*~*D*), the maximum axial stress experienced step change. The second stage (*D*~4*D*), the maximum axial stress decreases slightly, while the maximum principal stress fluctuates in a small range. When the dislocation reaches a certain value, which has a little effect on the pipe stress. However, it has obvious influence on the stress in the local bending region.

As shown in Fig.14, the curvature radius of PE pipe's displacement curve increases gradually and symmetrically at the bend with the increase of fault displacement. When the dislocation increases, the middle pipe segment in the two bends is gradually elongated and thinner, but the pipe is still smooth, and there is no shape mutation and energy concentration. Extracting the strain of the path, Fig.15 shows axial strain curves of non-pressure PE pipe under different displacements. The axial strain curve is basically centrally symmetric, but the right shift of the symmetric center near the compression side. It is obvious that the compression region is larger than the tensile region, and the maximum value of the compressive strain is greater than the maximum of the tensile strain. The shape is similar to "S" with a sharp angle, and the strain remains 0 after a distance from the fault, and the fault only affects the pipe segment. In Fig.16, the maximum axial stress approximately increases linearly and uniformly with the dislocation increases. The effect of fault displacement on the tensile (compression) is obvious in the local area of PE pipe.

Fig.17 shows the pipe displacements in the vertical direction near the fault plane. Because the pipe is extruded from the soil in X direction of the dislocation behavior, the PE pipe has a certain deformation. The displacement trend of the pipe in the Y direction has been shown previously. As the dislocation increases, the displacement range of the pipe in the Y direction also increases, and the increase is symmetrical about fault. The maximum displacement in Y direction appears in the middle section of the pipe. In order to establish the effect of dislocations on the cross section deformation of the pipe. the deformation degree of pipe with the flattening parameter (f) is characterized.

In the calculation of f, two special directions (X) and vertical (Y) are taken into account. Fig.18 and Fig.19 show flattening parameter curves of PE pipe through fault zone along the axis direction in cohesive soils. The change of diameter(ΔD_1) related to f_1 is measured with respect to the vertical pipe diameter (D_V), relations to $\Delta D_1=D_V-D$ and $f_1=\Delta D_1/D$. And the change of diameter (ΔD_2) related to f_2 is measured with respect to the horizontal pipe diameter (D_{H}), relations to $\Delta D_2=D_{\mathrm{H}}-D$ and $f_2=\Delta D_2/D$. PE pipe section distorted is uniformity and regularity. In contrast flattening parameter curves of PE pipe under different fault displacements, they are symmetric distribution, and the value of f increases gradually with the increase of fault dislocations. The flat degree in the horizontal direction is obviously greater than that in the vertical direction. The influence of fault dislocation is more obvious on the pipe horizontal diameter. In Fig.18, $f1$ descending about 1m near the fault plane is fast. Owing to dislocation extrusion of soil, PE pipe diameter decreases rapidly in the fault direction. Thus, the design criteria ensures that the performance limit of the deformation structure of buried PE pipe is 20%, considering the toughness of PE pipe, short-term deformation limit can reach 30%, and selecting 1.5 as the safety coefficient. At no inner pressure, the degree of $f1$ is as high as 17% when the fault reaches 4D. There is no destruction at fault region of PE pipe, but timely checking to prevent accidents is necessary. Fig.19 shows *f*2 increases rapidly from the distance to the fault plane about 1m. PE pipe diameter increases rapidly in the vertical direction of the fault. In the process of *f*2 reaching the maximum value, there is a small amplitude fluctuation in the high stress zone. Compression stress and bending stress appear in the pipe wall. Moreover, the bending stress is a function of the difference between the horizontal and vertical soil pressures. The greater the pipe flexibility, the greater the possible deformation is. With the increase of pipe deformation, the reaction force in the vertical direction gradually shifted from the active to the passive. At a certain stage, the soil pressure will reach a vertical and horizontal balance. At this point, the pipe mainly bears the effect of cyclic compressive stress, and the excessive compressive stress will cause the pipe to buckling[3].

4.1.2 Effect of layer properties

Fig.20 shows principal stress distribution of non-pressure PE pipe in the fault area. The distributions of high and low principal stress regions on the pipes embedded in four kinds of soils are obvious. On one side of the fault direction, due to the contact extrusion of PE pipe and soil, the zone of high principal stress is ovale. However, in the opposite side of the soil movement, there is a low stress zone, because the pipe and soil are not contact with the their gap. Deformation of PE pipe in the sand soil is smaller, and the maximum principal stress is smaller, but the region of the high principal stress is larger under the same fault displacement. Nevertheless, the deformation and stress distribution of the PE pipes in the other three kinds of soils are similar.

The principal stress curves along the PE pipe segment and stress curve in the ring direction at the maximum value are shown in Fig.21. The principal stress in the pipe is slightly fluctuating at the area far away from the fault plane. Overall, the maximum stress of PE pipe embedded in sand soil is the largest, followed by silty clay, cohesive soil, and loess. In the range of 0.5m near the fault plane, the stress increases rapidly to about 25MPa. The principal stress of PE pipe is embedded in loess is the largest, and that in sand is the smallest. The maximum principal stress in loess farther away from the fault plane. Then, the stress restores to about 2.5MPa near the fault plane 0.75m. The stress recovery area of PE pipe embedded in loess is longer than that in other soils. So, the strike-slip fault has a greater impact on the PE pipe in the sand. However, the fault movement causes the maximum stress of PE pipe in the loess is larger than that in other soils. Finally, the principal stresses keep stable. The principal stress of PE pipe in the sand is still the largest, and the minimum value is in the cohesive soils in the stable region.

Taking the hoop principal stress curve at the point of the maximum stress, the with curve regularity in the three kinds of surrounding soils are similar except sand. The stress is bigger than 20MPa in the range over 150°, after then stress decreases rapidly in the range of 30 ~60°respectively. Finally, in the range within 120°, it is stable in the low principal stress about 5MPa. The whole stress ring curve of the PE pipes embedded in three soils changes obviously than in loess. Nevertheless, that of the PE pipes embedded in loess is approximate circular, the maximum principal stress appears at only one point, and the stress reduces uniformly in the range of

150°respectively. Because the soil properties are different, especially the cohesion force. Cohesive force of the loess is zero, and the smaller value is used to the finite element calculation. In the case of fault, the ultra-low cohesive of loess is easily deformed. In the fault area, uniform deformation of soil makes homogeneous change of hoop stress on the PE pipe. Because the cohesive force of cohesive and sandy soils is slightly higher than the loess, which has a certain inhibition on pipe deformation in the fault area. The energy accumulate on the contact surface which result in the high stress area. Once the contact surface of the pipe separates, PE pipe energy release, the principal stress decreased rapidly along the circumferential. So that the low stress stable region appears opposite to the high stress.

As shown in Fig.22, these paths of the special position on the motion direction of the layer (X-axis) and the circumferential path of the strain maximum is highlight. The axial strain distribution of these paths are obvious. The tension side presents a high strain zone, and the compression side is in a low strain zone. The two sides are symmetrical. Fig.23 shows the axial strain curves on the paths. These axial strain curves are approximately sine curve, and centrally symmetric on fault plane. The change of axial strain area of PE pipe is large in the loess, at about 1.5m on both sides of the fault plane. Compared with other three kinds of surrounding soils, the maximum axial strain is farther away from the fault plane in the loess, and the axial strain of the PE is smallest. In addition, Fig.23 also shows the axial strain of ring of the PE pipes at marking. The circumferential strain curve of PE pipe in the loess is slowly and evenly, and the maximum difference is about 0.04. Moreover, the curve changes of pipe in other three kinds of soils are concentrated on 90°on both sides, and the maximum difference is about 0.08. It is almost two times as high as the maximum difference.

Fig.24 and Fig.25 show the flattening parameter curves of PE pipe embedded in the different soils in the special directions include horizontal (X) and vertical (Y) respectively. Deformation regularity of these curves is similar but with obvious differences. Considering the deformable degree of pipes in various surrounding soils after the fault, the deformation rate of cross section (*f*1 and *f*2) is around -1.5% in 3m on both sides of the fault palne. Small necking occurs in the pipe because of a certain tension in this area. The flattening parameter curve is symmetrical on the left of the fault plane, and the changes greatly in 1m on both sides of the fault plane. The change of flattening parameter in the cohesive soils is the largest, followed by sandy soils, silty clay and loess. In the middle area, the *f*1 curve is inverted triangle. In this direction, the diameter of PE pipe decreases monotonically from both sides to the fault plane. The *f*2 curve assumes "W" with the highest peak in the middle. In this direction, the PE pipe diameter increase first and then decrease, next increase to maximum from both sides to the fault plane.

When the fault dislocation is 4*D*, the flattening parameter *f1* in the loess is only 6% in the horizontal direction. In addition to the sand, *f1* in other soils up to 14%~18%. However, the deformation rate is not exceeded the performance limit of 20% deformable structure about the buried PE pipe defined in the previous article, and it is safe. Compared with *f1*, the flattening coefficient of the pipe is much smaller in vertical direction. The *f2* maximum is only 3.5% in four kinds of soils, and the diameter of PE pipes only changes slightly in Y direction. The greater the cohesive force of the soil around the PE pipe, the greater the section deformation of the pipe in the strike-slip fault area. Therefore, it is necessary to check on the PE pipe and safety assessment after destruction of fault in large cohesive soil.

4.2 Mechanical analysis of pressurized PE80 pipe

4.2.1 Effect of fault dislocation

In the actual conditions, when normal gas transportation, the influence of the inner pressure on the PE buried pipe cannot be ignored. According to the requirements of the maximum working pressure of PE80, it is not greater than 0.8MPa. Taking a PE80 pipe with diameter (*D*) of 110mm and the inner pressure of 0.8MPa as an example.

As shown in Fig.26, the displacement curves of pressurized PE pipe appear small fluctuation on one side of the fault plane, which can firstly increase and then decrease. The pipe subjects to different certain degree of tensile deformation and displacement in the area where the pipes and the soil have detached. Fig.27 shows the axial strain curves of the pipe under the different dislocations. The axial strain changes regularly with the increase of the dislocations. The axial strain rate of PE pipe increases, and the extreme value of axial strain increases in this pipe segment. Fig.28 shows the maximum axial strain curve, which is approximately linear.

Fig.29 shows the axial stress curve of pressurized PE pipe under different fault displacements. The fault displacement has a obvious influence on the axial stress in middle area. With the increasing of fault dislocation, axial stress increases in the far from the fault plane. The axial stress on the fault plane is zero. The greater dislocation, the larger the area affected by the fault is, and the pipe is hardly affected by the fault after a certain distance. As the Fig.30 shows, in the process of *D* to 2*D*, the maximum axial stress of the pressurized PE pipe is rapidly increasing, and little difference of the maximum axial stress under the two pressures. The soil displacement had a great effect on maximum axial stress in this part of dislocation. However, the maximum axial stress remains constant after the displacement exceeds 2*D*.

Due to the dislocation of the soil, the pressurized pipe subjects to both internal and external pressures, which will cause pipe deformation. Considering the extrusion between internal pressure and soil, the influence of fault displacement on the deformation degree of PE pipe by analyzing the change of cross-section of PE pipe in XY plane.

Fig.31 and Fig.32 show the cross-section deformation rate of the pressurized PE pipe passing through the clay fault under different disaplcements. Considering the deformation rate of the above five cases, *f1* changes rapidly at 0.5m from the fault plane, until it reaches the extreme value at the fault plane, and then changes symmetrically to form "V". In other words, the closer to the fault plane, the X-axis diameter decreases rapidly, and that is minimized at the fault plane.

However, the *f2* increase from the same position, but there are different degrees of attenuation at 0.4m from the fault plane. Moreover, the attenuation percentage increases gradually and the regularity is more significant with the increase of fault dislocation. The curve of *f2* is approximately symmetrical on the small peaks on both sides of the fault plane. That is to say, the Y-axis diameter increases rapidly and weakly attenuates at the closer to the fault plane. The maximum flattening parameter is up to 22% in the process of the fault displacement increasing. The deformation rate exceeds the deformation limit of 20% about the buried PE pipe in the previous chapter with selecting safety factor of 1.5, and it is a dangerous. In the process of strike-slip fault, the *f* in the X-axis direction is larger than that in the Y-axis direction, and the PE pipe is dangerous earlier in the fault direction. Therefore, it is very important for safety inspection and time maintenance of the gas pressurized PE pipe in the easy fault zone.

4.2.2 Effect of layer properties

The axial stress distribution of PE pipe segment carrying fluid pressure load as shown in Fig.33. Under four kinds of soils, PE pipes with 0.8MPa exhibite the same rule.

Due to extrusion of PE pipe-soil system, the principal stress of PE pipe on the contact surface with soil gradually increases, while it remains lower on the side of gap with soil. Under the same conditions, PE pipe shows a smaller deformation and high-stress zone in loess. It indicates that the sand soil has a small extrusion effect on the pipe, and the sand movement adapts to the pipe deformation. Compared with the non-pressure PE pipe, the inner pressure has a little effect on the stress-strain of the pipe in the fault zone.

Fig.34 shows von Mises stress of PE pipe segment in loess layer, including the stress distribution in two axial paths and a circumferential path of the maximum stress point. There is a circular low stress area at the center of the fault palne. The symmetrical distribution of oval stress ring on both sides of the fault plane appears, where stress decreases gradually from inside to outside. Due to the contact and extrusion of the pipe-soil system in the loess fault, the high-stress zone appears in both of tension and compression sides, and the energy accumulation occurs. On the PE pipe side, a strip of low-stress band appears because of the energy release.

As shown in Fig.35, the stress of the path on the tensile side of the PE pipe experiences a large fluctuation. Within 1.5m from the fault plane, the principal stress rapidly increases to 25~28MPa and then rapidly decreases to 0. After slight fluctuation, the principal stress is stable near 3MPa. The maximum stress of the PE pipe in loess appears the location that far away from the fault plane, and the main stress has a wider range, but the maximum is the lowest. In the circumferential stress curve of PE pipe, that in loess is different from the other. Without region of sustaining high stress, uniform and slow down in 120° on both sides, within about 120° stable in the low main stress. In the other three kinds of soils, the PE pipe can maintain about 150 ° high stress zone, and in the range of 30° on both sides of the rapid decline.

As shows in Fig.36, the axial strain regularitys of each paths at the pressurized PE pipe are same with that at the non-pressure PE pipe. They are approximately sine curves and symmetry on the fault plane. In the loess, the influenced area of axial strain is larger, and the maximum value of axial strain farther away from the fault plane. The circumferential strain curve of PE pipe in loess appears circular, that in other kinds of soils shows shape of peach.

As shown in Fig.37 and Fig.38, $f1$ and $f2$ curves regularity of PE pipe with 0.8MPa in different soils are the same with that of non-pressure PE pipe. Therefore, the inner pressure of 0.8MPa have a little impact on the cross-section deformation of PE pipe under the strike-slip fault. As in the condition without pressure, the maximum of $f1$ in the fault (X-axis) direction is about 6 times that of $f2$ in the vertical (Y-axis) direction. That is to say, the deformation of the PE pipe section in the fault direction is much greater than that in the vertical direction in the slip fault zone. From the flattening parameter data of the PE pipe outside the fault plane around 2m, the stability of flattening parameter is similar in both directions of the PE pressurized pipe, and $f1$ and $f2$ are maintained at about -0.1%. Compared with non-pressure pipe, both $f1$ and $f2$ of PE pipe increase in this area. The existence of inner pressure can inhibit a level of pipe deformation. The f curves of symmetry distribution have significant changes in the fault plane on both sides of 1m range. Among them, the change of flattening parameter about PE pipe is the largest in cohesive soils, the result in silty clay is similar to that in sandy soils, and the loess is the smallest. As with non-pressure PE pipe, the $f1$ curve shows an inverted triangle, and the $f2$ curve is “W” in the middle region, but the f curves have a large fluctuation in the case of pressurized PE pipe. Taken together, these results suggest that the inner pressure of the PE pipe has an unstable effect on the flattening parameter in near the fault plane.

When the dislocation up to $4D$, the $f1$ of PE pipes with inner pressure increase to 16%~18% in the three kinds of soils, the loess excepted. It does not exceed the deformation texture limit of the buried PE pipe of 20%, which is defined by this article. The inner pressure has a little effect on the pipe deformation, so it cannot significantly prevent cross-section deformation. At this time, the maximum *f* of PE pipe in loess is only 6%, and it is sure to be safe. Therefore, the real gas pressure in the working is considered to ensure the accuracy of the results in the strike-slip fault. Notably, the difference of the surrounding soil has a great influence on the deformation and failure of the pressurized PE pipe.

4.2.3 Effect of pipe size

In the actual projects, the PE pipes have a variety of sizes for gas transmission. Referring to *Gas Buried Polyethylene (PE) Pipe System for Gas Use* GB15558, combining with the standard size ratio of PE80 pipe used for gas are 11 and 17.6 respectively. The pipe specifications for the three groups of PE pipes are shown in Table 3. In the model of 2m × 1m × 20m, setting the depth of 0.5m PE pipes to analyze the influence of different sizes on strength and deformation of pressurized PE pipes in the same zone. Considering the appropriate fault displacement of the pipe specifications, the fault dislocation is 0.44m. Corresponding to 50% of the maximum operating pressure $p_{\max}$ of the pipe, the same operation pressure of PE pipes is 0.4MPa to ensure safety. The standard dimension ratio of a fitting (*SDR*) is the geometrical terminology of the PE pipe, which is the ratio of the nominal diameter to the nominal wall thickness of the pipe, also called the diameter thickness ratio[1].

The design of gas-engineering takes allowed standard for foundation, as far as possible, reduces the expense of engineering. Selecting the slender pipe, based on guaranteeing the flow of gas pipe network. Three groups of PE80 pipes with different diameters are listed. Displacement curves of PE80 pipes with different sizes are shown in Fig.39. These curves show symmetry about the fault center. Along the pipe segment, the displacement transits from -0.22m to -0.22m in fault area. Displacement curves of PE pipes with different thicknesses coincide nearly, indicating that the thickness has a little effect on the pipe displacement. For PE pipes with the same *SDR*, the larger the diameter, the larger the transitional area and the smoother the curve of transition. Because a wider range of soil deformation causes the extrusion from the contact surface between PE pipe and soil in the fault area when the increasing of pipe diameters. Importantly, the thinner pipe are affected more easily by the strike-slip fault.

Fig.40 show the axial stress curves of PE80 pipes with two groups sizes. All curves presenting approximately sinusoidal along the pipe segment. The axial stress of the PE pipe with the same diameter is not significantly different. The greater the *SDR*, the greater the stress change is. Because the reduction of the wall thickness will weaken the pipe strength. However, the effect scope is the same. The stress distribution appears an oval on the tension side of the PE pipe, and symmetry on the fault plane. Axial stress of PE pipes with the same *SDR* is difference. The greater the diameter, the larger affected areas and the smaller the degree. Because a larger the pipe diameter results in a greater the contact surface of the pipe and soil. The the high stress produced by the motion extrusion will pass around to a large extent under certain dislocations. In the case of the same fault, the diameter has a certain effect on the axial stress and strain. A larger diameter may results in a smaller stress and strain.

With the increase of fault displacement, the maximum principal stress curves of PE80 pipes with different sizes appear parabolic shape as shown in Fig.41. During the increasing of fault displacement from 0 to 0.44m, the maximum principal stress curves of PE pipes with *SDR* 17.6 are greater than the curves of pipes with *SDR* 11. In other words, the maximum principal stress of the PE pipe with a larger *SDR* is larger. When *D* is 110mm, the maximum principal stress curves of the two *SDR* are quite different. When the fault dislocation is about 2.8m, the difference is up to 5MPa. The maximum principal stress curves of the PE80 pipes with three diameters in the same *SDR* are made. The stresses vary greatly owing to different diameters. With the increase of fault dislocation，the maximum principal stress increases, but the slower the increase rate is. Besides, the larger the diameter, the smaller the maximum principal stress is. When the fault displacement is 0.44m, the maximum stress of PE pipes up to 19MPa ~28MPa.

As shown in Fig.42, in the range of 2m on both sides of the fault plane, the tendency of axial strain curves is similar to the axial stress curves. There are significant differences and obvious trends between axial strain curves of PE80 gas pipes with different *D*. With the increasing of the diameter, the period increase and the curve amplitude decreases. In the process of fault movement, pipe-soil contact surface is separated on one side, but the extrusion on the other side leads to a large axial strain on the PE80 pipe. As the diameter increases, the affected length of pipe increases in fault zone, but the strain intensity is weakened. Compared with the stress tendency, the diameter has a similar effect on the axial strain in the same slip fault. When the *SDR* is 11, the symmetry center deviates from the fault plane.

The max axial strain curves are shown in Fig.43. The larger the *SDR* of PE pipes, the greater the change proportion of the max axial strain and the steeper curves. The max axial strain curves laws of PE pipes with different diameter are obvious, and the maximum axial strain increases as the parabolic shape with the increase of the fault dislocation. With the increasing of the diameter, the maximum axial strain increases. When the fault dislocation is within 0.44m, the maximum axial strain is greater than 2.5%. And the growth rate is also greater, the maximum change is over 1%. Therefore, the slender PE pipes should be reasonable safety monitoring and regular maintenance.

When the fault displacement is 0.44m, the flattening parameter *f*1 and *f*2 of PE80 pipes with different sizes in 0.4MPa internal pressure are shown in Fig.44 and Fig.45, respectively. The *f*1 curves appear rapid reduction and rapidly rising in the 2m range on both sides of the fault plane. The fluctuation is approximately symmetrical to the fault plane. There are obvious differences about *f*1 curves with the different *SDR* near the fault plane, and the *f*1 curve is always below when *SDR* is 17.6. For example, when diameter of PE pipe is 110mm, the minimum *f*1 of *SDR*=11 is as low as -6%, that of *SDR*=17.6 pipe is about -8%. Under the same diameter, the *f*1 difference between the two groups of *SDR* is within 3%. In the fault zone, squeezing ground gives rise to flattening PE pipes with three diameters. And the *f*1 curves are symmetrical on both sides, and there is a valley at the fault plane. When *SDR* of PE pipe is 17.6, the minimum *f*1 when *D*=75mm is as low as -14%, the difference between with that when *D*=160mm is about 11%. The wall thickness has a little effect on the flattening parameter *f*1. The deformation rate of the pipes is symmetry of both sides of the fault plane, and the effect of the pipe size on the deformation is obvious.

In the vertical direction, the trend of *f2* curves about two kinds of *SDR* is a clear difference with the curves of *f1* in the fault direction, as shown in Fig.45. Different from the simple trough of *f1* curves, *f2* curves fluctuate slightly within 0.5m of the fault plane, but the degree is not large. Forming a "W" shape symmetrical about the fault plane, these data are consistent with the notion that deformation of the PE pipe is unstable because of necking caused by the tension of the flexible pipe. When the diameter of PE pipe is 110mm, the *f2* curve of *SDR* 17.8 is always greater than that of *SDR* 11, and the volatility is similar. When *SDR* of PE pipe is 11, the maximum difference of *f*2 curves is about 3.5% between three pipes in the analysis section. That is, compared with the fault direction, the pipe deformation is smaller in the vertical direction. However, the characteristics of *f2* curves are quite different with different pipe diameters. The smaller the diameter, the larger the oscillation of the *f2* curves is. When the pipe diameters are 110mm and 75mm, the *f2* value increases from -1% to 2% from two sides to the fault plane, which indicates that pipe diameter gradually increases from less than the original diameter to more than the original diameter in the vertical fault direction. In the fault region, the diameter has a great influence on pipe deformation . Therefore, it also has a great influence on the loading capacity of the PE gas pipe. In summary, the safety measures of slender pipes should be given to prevent from the damage of the PE gas pipe network in service.

5 Conclusions

This paper has examined the mechanical behavior of buried PE gas pipe under the strike-slip fault movement. Under the slip fault, the strength of buried non-pressure and pressure PE pipe with a diameter of 110mm was investigated, and the judgment of pipe failure is made, and then the safety evaluation suggestion is put forward. The results show that:

(1) The buried PE pipes under no pressure and 0.4MPa were studied. The study indicates that the inner pressure has a little effect on the strength of PE pipe under strike-slip fault, but it has a less resistance to the deformation of PE pipe. Therefore, the appropriate inner pressure can play a certain role to hinder the deformation of PE pipe in the fault zone.

（2）The overall flatness curve of buried PE gas pipe under slip fault is symmetrical about the fault plane and the deformation rate increases with the fault dislocation increases. The flattening parameter in fault direction is obviously higher than that in vertical direction. As a result, the deformation of the buried flexible pipe is distorted due to horizontal displacement, which is also affected by the vertical direction of soil around the pipe. Therefore, it is extremely important to predict the earthquake fault zone and fault hazard series.

（3）The deformation of PE pipe under four kinds of soils in the slip fault area is regular but the difference is obvious. The flatness changes greatly within 1m around the fault plane. The change of flattening parameter of PE pipe in cohesive soil is the biggest, followed by sandy soil, then silty clay, and the last is loess. Because the different properties of the soil around the PE pipe in the slip area results in different deformation of soil and the pipe section. Therefore, it is necessary to do safety testing of the deformation and destruction of PE pipe buried in the soil with special properties.

（4）When the fault dislocation is 0.44m, the larger the *SDR* of PE80 with the inner pressure 0.4MPa, the higher the flattening parameter of the pipe and the weaker the resistance deformation of pipe with the same diameter. With the pipe diameter increases, the flattening parameter of the pipe diameter decreases, and it is strong for the resistance to pipe deformation with the same diameter-thickness ratio. In contrast, the diameter has a significant impacts on the flattening parameter of the pipe diameter. Due to the flexible pipe under the tension appears a certain degree of necking phenomenon, the pipe diameter changes unstably. Therefore, PE pipe with a higher *SDR* and a smaller diameter for transporting gas should be properly monitored.

Acknowledgements

This work is supported by Scientific Research Starting Project of SWPU（No.2017QHZ011）, State Key Laboratory for Strength and Vibration of Mechanical Structures（No.SV2017-KF-08）, Key Laboratory of Superlight Materials & Surface Technology (Harbin Engineering University), Ministry of Education, Chengdu science and technology program (2016-HM01-00306-SF) and Nanchong science and technology program (NC17SY4018).

References

[1]Sun D, Yao Z, Zhao Z. Development trend of gas business in China. *ChengShi RanQi*, 2006, (09):35-40

[2]Khelif R, Chateauneuf A. Reliability-Based Replacement of Polyethylene Gas Pipeline Networks. *Arabian Journal for Science and Engineering*, 2014, 39(11): 8175-8185

[3]Zhang J, Xie J. Investigation of Static and Dynamic Seal Performances of a Rubber O-Ring. *Journal of Tribology*, 2018,140(4), 042202.

[4]Younan M Y A, Radwan S A. Experimental Investigation Into the Fracture Toughness of Polyethylene Pipe Material. *Journal of Pressure Vessel Technology*, 2005, 1(127):850-868

[5] Jin S, Hou L, Yang Y. Risk Assessment Index System of PE Gas Pipeline Based on Kent Scoring Method. *Gas & Heat*, 2014, (03):88-91

[6]Zhou L. Study on Risk Assessment Technology of Third-party Excavation Damage in Urban Gas Pipelines. *Southwest Petroleum University*,2017

[7]Liang Z, Zhang J, Han C. Study on Mechanical Behavior of Oil and Gas Pipelines under Typical Geological Disasters. *Science Press*, 2016:1

[8]Guo Y，Fu X，Meng T. Risk Assessment of City-gas PE Pipeline Based on Variable Weights and Grey Theory. *Pressure Vessel Technology*, 2015, (03):59-65

[9]Guo X. The Research of Safety Issues on PE Pipe Transporting CBM Under Traffic Loads. *Chongqing University of Science and Technology*, 2015

[10]Luo X, Lu S, Shi J. Numerical simulation of strength failure of buried

polyethylene pipe under foundation settlement. *Engineering Failure Analysis*, 2015, 48:144-152

[11]Ma J.. Numerical simulation of strength of buried polyethylene pipe under typical complex loading. *Zhejiang University*, 2013

[12]Tafreshi S N M, Khalaj O. Laboratory tests of small-diameter HDPE pipes buried in reinforced sand under repeated-load. *Geotextiles and Geomembranes*, 2008, 26(2):145-163

[13]Esmaeili-Bafghi-Karimabad A, Ghanbari D, Salavati-Niasari M, et al. Photo-catalyst tin dioxide: synthesis and characterization different morphologies of SnO 2, nanostructures and nanocomposites. Journal of Materials Science Materials in Electronics, 2015, 26(9):1-9.

[14]Suleiman M T, Coree B J. Constitutive Model for High Density Polyethylene Material: Systematic Approach. *Journal of Materials in Civil Engineering*, 2004, 6(16):511-515.

[15]Xu C. Prediction of Creep-rupture Failure Time of HDPE Pipe. *Zhejiang University*, 2012

[16]Shareghi B, Farhadian S, Zamani N, et al. Investigation the activity and stability of lysozyme on presence of magnetic nanoparticles. Journal of Industrial & Engineering Chemistry, 2014, 21(3):862-867.

[17]Mazloom F, Masjedi-Arani M, Ghiyasiyan-Arani M, et al. Novel sodium dodecyl sulfate-assisted synthesis of $Zn_3V_2O_8$, nanostructures via a simple route. Journal of Molecular Liquids, 2016, 214:46-53.

[18]Shareghi B, Farhadian S, Zamani N, et al. Stability and enzyme activity of lysozyme in the presence of Fe_3O_4, nanoparticles. Monatshefte für Chemie - Chemical Monthly, 2016, 147(2):465-471.

[19]Yousefi M, Gholamian F, Ghanbari D, et al. Polymeric nanocomposite materials: Preparation and characterization of star-shaped PbS nanocrystals and their influence on the thermal stability of acrylonitrile–butadiene–styrene (ABS) copolymer. Polyhedron, 2011, 30(6):1055-1060.

[20]Salehabadi A, Salavati-Niasari M, Ghiyasiyan-Arani M. Self-assembly of hydrogen storage materials based multi-walled carbon nanotubes (MWCNTs) and Dy 3Fe5O12, (DFO) nanoparticles. Journal of Alloys & Compounds, 2018, 745.

[21]Zhou X, Qian Q, Yang H. Strength Criteria of Deep Rock Mass. *Chinese Journal of Rock Mechanics and Engineering*, 2008, (01):117-123

[22]Zhang J., Zhang L., Liang Z. Buckling failure of a buried pipeline subjected to ground explosions. *Process Safety and Environmental Protection*, 2018,114:36-47.

[23]Xiao Z, Huang X.. Friction System between Buried Hot Oil Pipeline and Surrounding Soil. *Special Structures*, 1990:43-46

[24] Fujikake M, Fukumura M, Kitao K. Analysis of the electrofusion joining process in polyethylene gas piping systems. *Computers & Structures*, 1997, 5-6(64):939-948

[25]Sun X. Polyolefin Pipe. *Material science and Engineering Publishing Center of Chemical Industry Press*, 2002

[26]Vazouras P., Karamanos S. A. Structural behavior of buried pipe bends and their effect on pipeline response in fault crossing areas. *Bulletin of Earthquake Engineering*,

2017, 15(11):4999-5024

[27]Yang H., Ji Y. Discussion on Methods of Selecting Gas Pipeline Diameter. Hanghai Gas, 2015, (02):15-1717141

[28]Zhang J., Xie R., Zhang H.. Mechanical response analysis of the buried pipeline due to adjacent foundation pit excavation. *Tunnelling and Underground Space Technology*,2018，78：135-145.

[29]Vazouras P., Karamanos S. A., Dakoulas P. Mechanical behavior of buried steel pipes crossing active strike-slip faults. *Soil Dynamics and Earthquake Engineering*, 2012, 41:164-180

Table 1 Performance parameter of PE pipe

Material	Density **Error! Reference source not found.** (kg/m3)	Elastic modulus *E* (MPa)	Yield strength **Error! Reference source not found.** *y* (MPa)	Poisson's ratio *u*	Minimum required strength
PE80	951	1512	26.9	0.45	8MPa

Table 2 Mechanical parameters of soil

Type	density **Error! Reference source not found.** (kg/m^3)	Elastic modulus E (MPa)	Poisson's ratio u	Cohesion c (KPa)	Fiction angle **Error! Reference source not found.**(°)	Dilation angle θ(°)
cohesive soil	1960	18	0.35	22	34	0
silty clay	1960	10	0.35	22	25	0
sandy soils	1800	33	0.44	24.6	11.7	0
loess	1400	20	0.35	5	15	0

Table 3 Pipe specification

Number	nominal diameter Dn / mm	$SDR11$ Maximum working pressure ≤ 0.8 MPa	$SDR17.6$ Maximum working pressure ≤ 0.482 MPa
		Nominal thickness t_1 / mm	Nominal thickness t_2 / mm
1	75	6.8	4.3
2	110	10	6.3
3	160	14.6	9.1

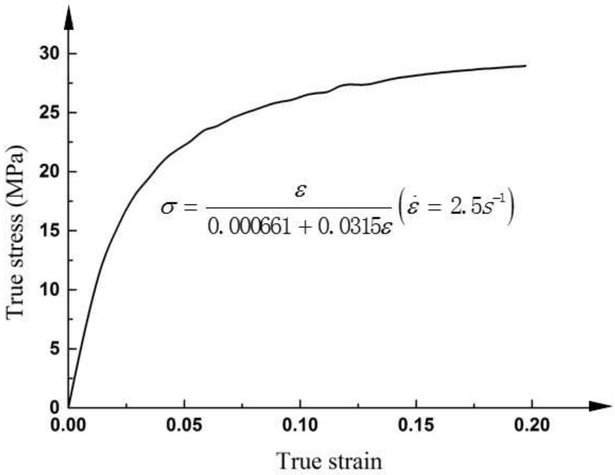

Fig.1 The true stress-strain curve of pipe PE80 ($\dot{\varepsilon} = 2.5s^{-1}$)

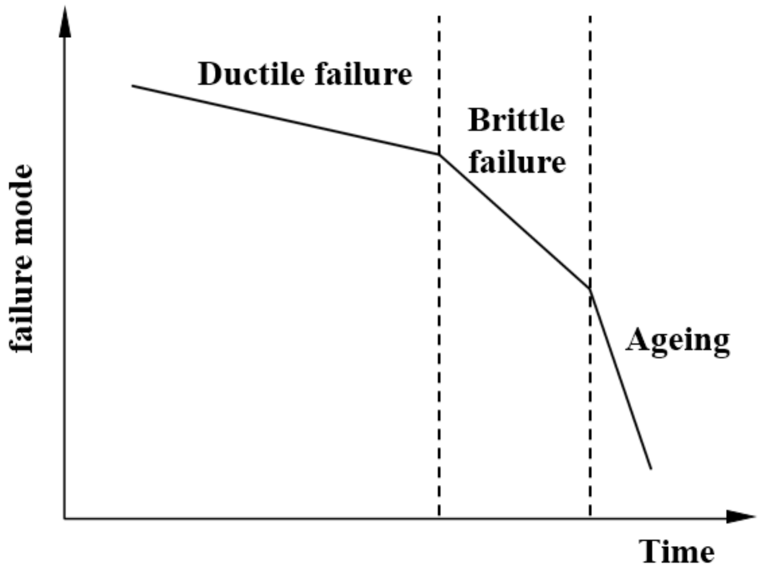

Fig.2 Failure mode of the PE pipe

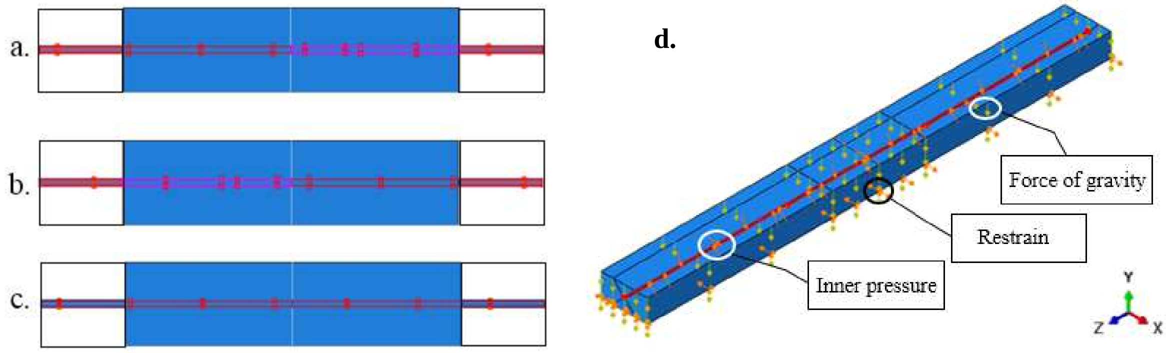

Fig.3 Contact and boundary of pipe-soil system

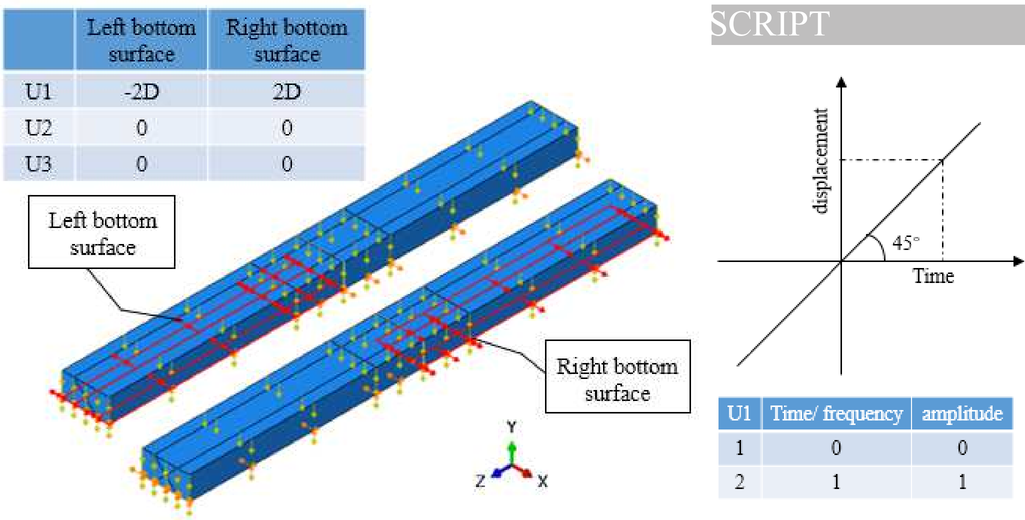

Fig.4 Load and motion settings of pipe-soil system

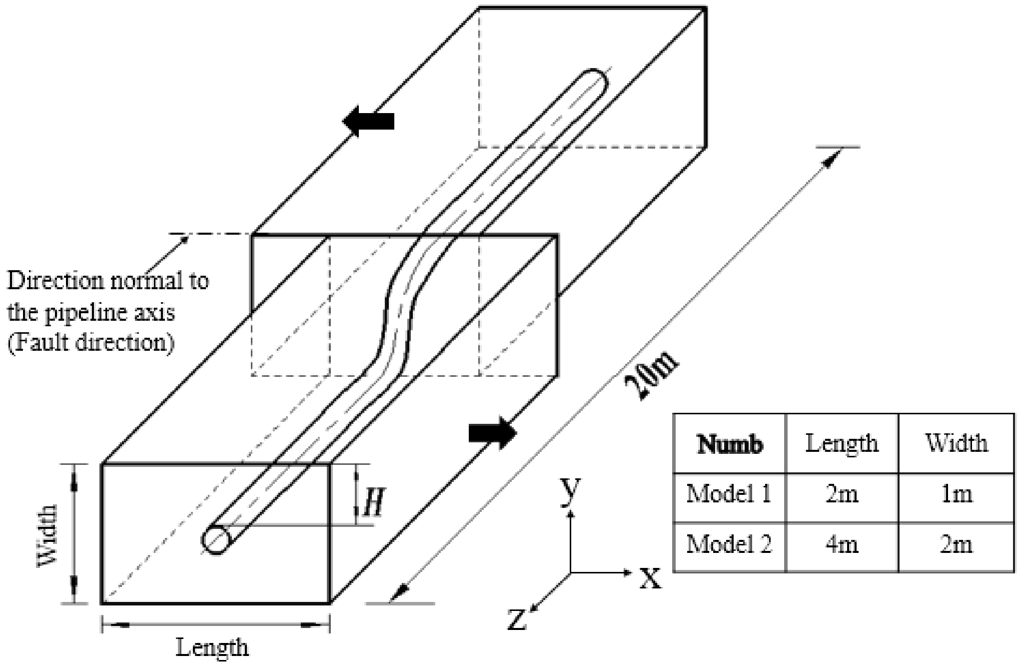

Numb	Length	Width
Model 1	2m	1m
Model 2	4m	2m

Fig.5 Schematic of a PE pipes crossing strike slip fault

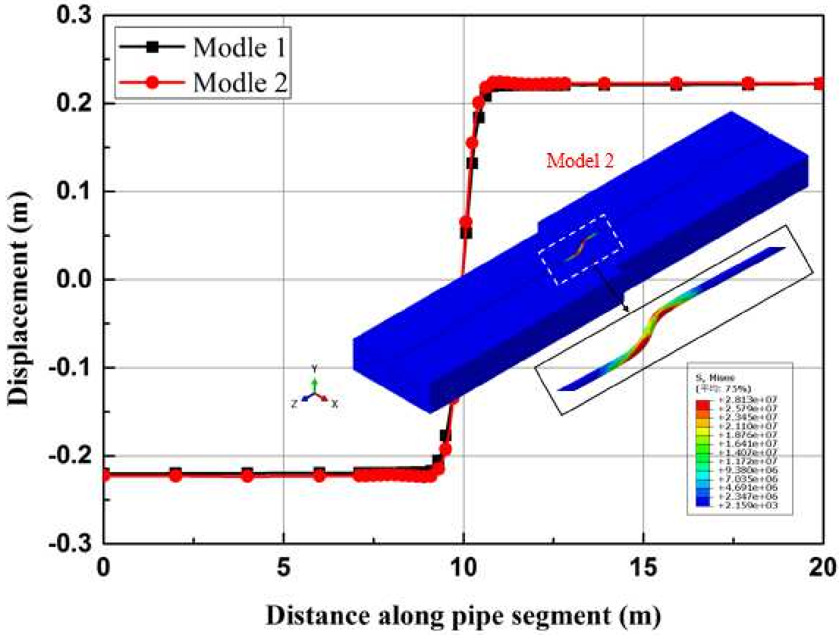

Fig.6 Deformation curves of PE pipes in different models

(a)

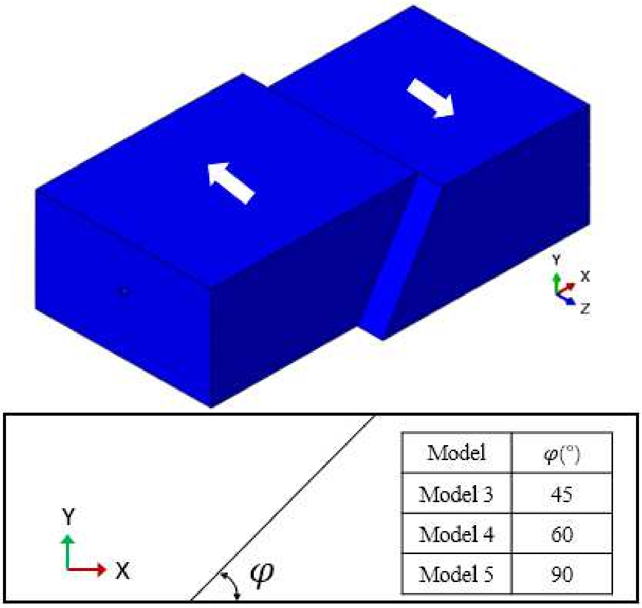

Model	φ(°)
Model 3	45
Model 4	60
Model 5	90

(b)

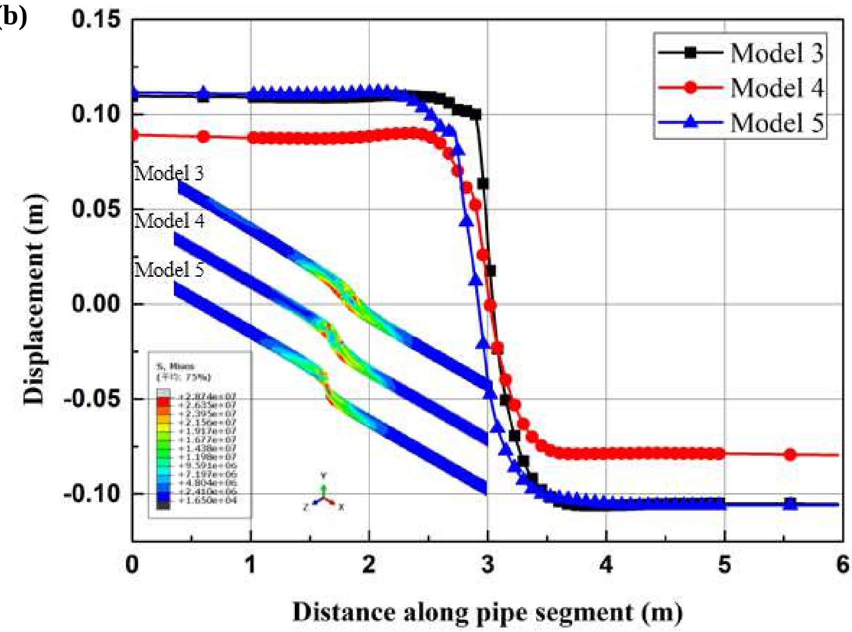

Fig.7 Analysis of PE pipe with dip angle of strike-slip fault. (a) Simple models. (b) Deformation curves of PE pipes

(a)

(b)

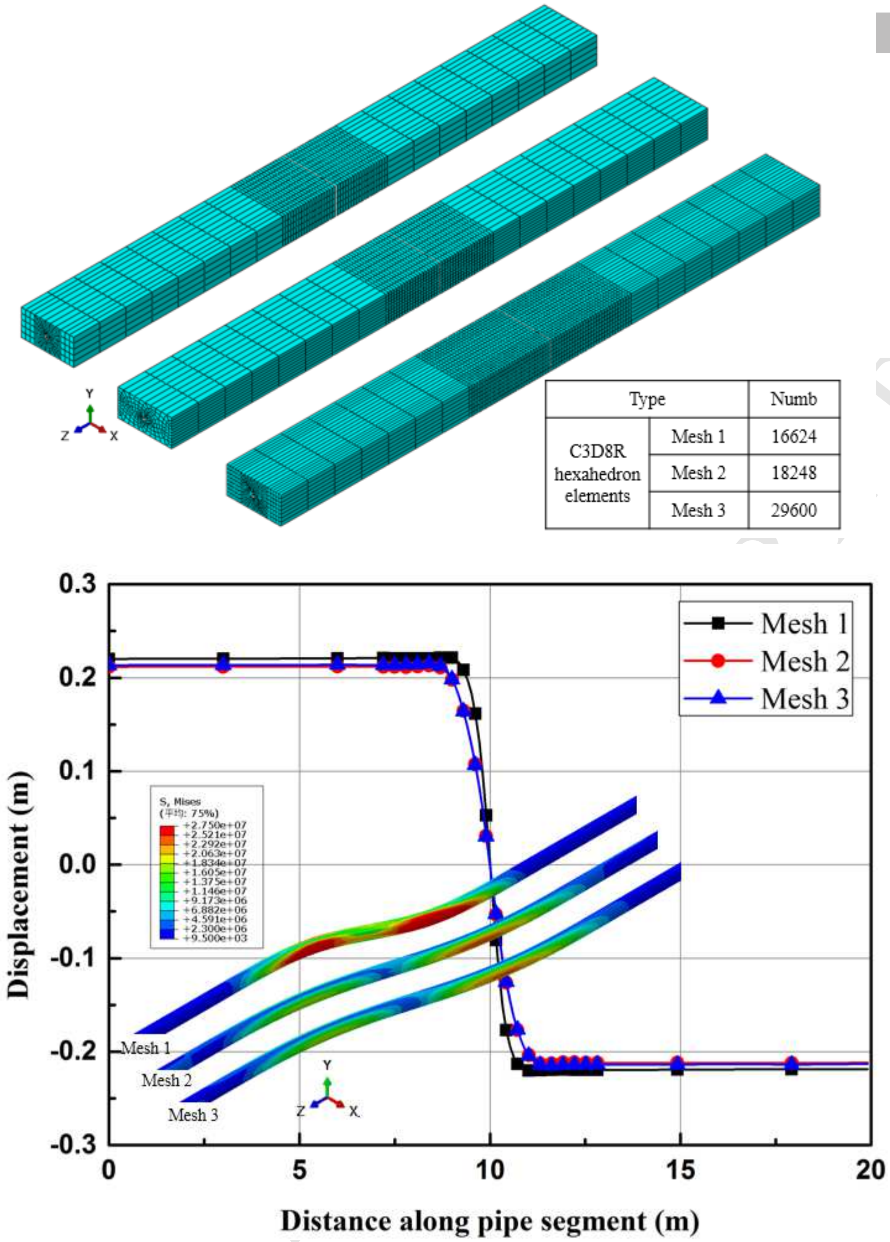

Fig.8 Analysis of PE pipe with different mesh. (a) Different mesh number. (b) Deformation curves of PE pipes

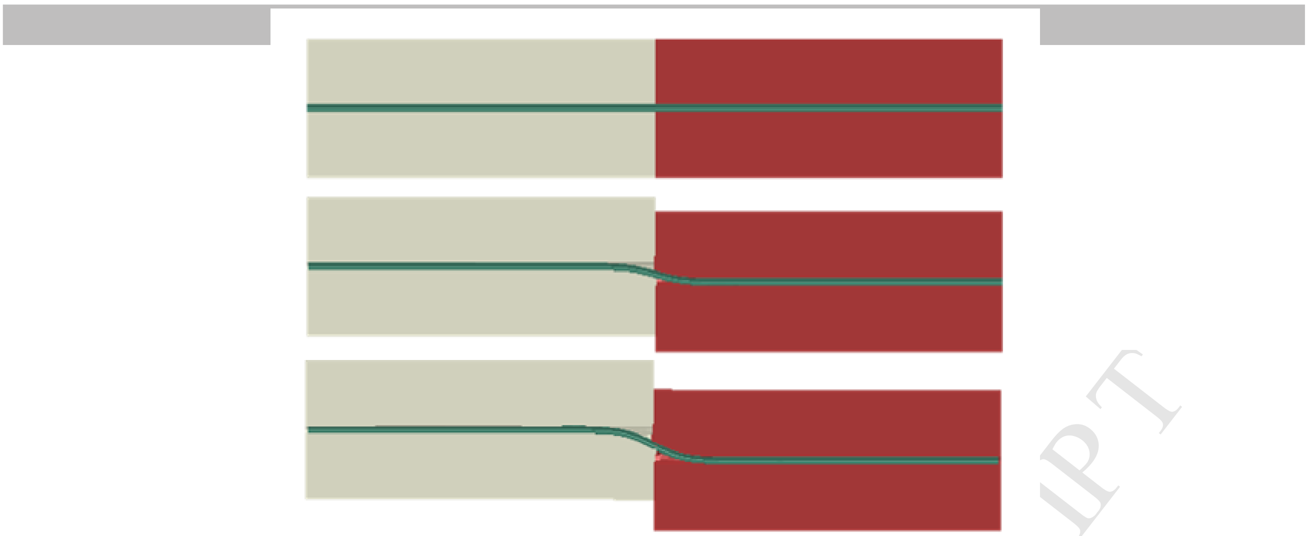

Fig.9 Deformation of pipeline-soil system under strike-slip fault

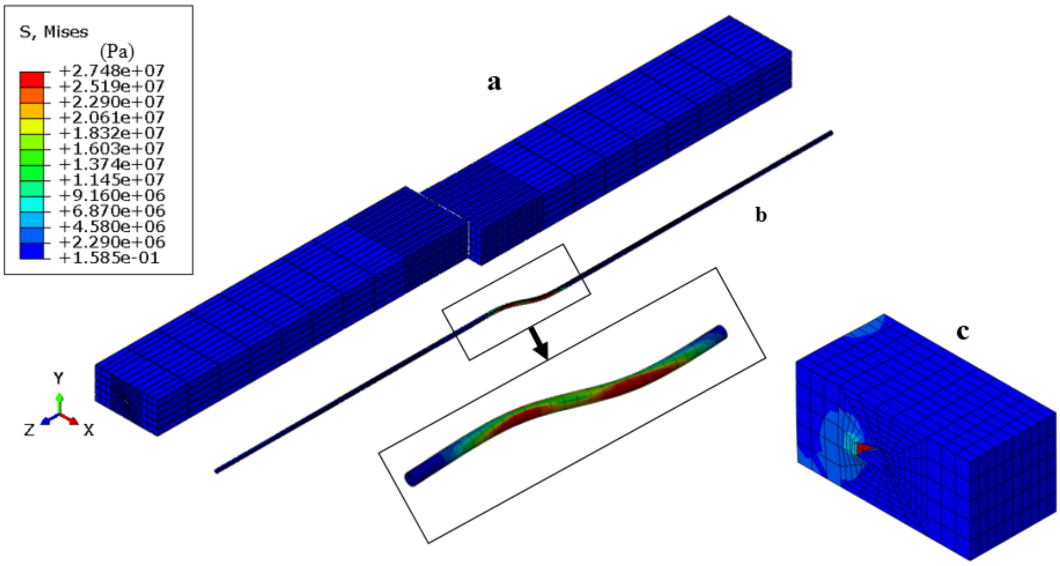

Fig.10 Stress distribution of the whole model under strike-slip fault

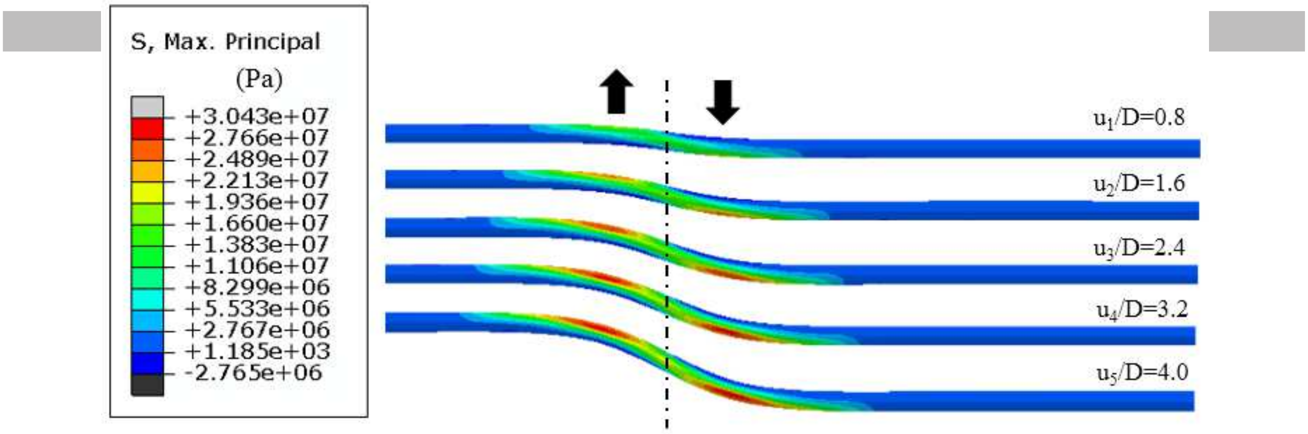

Fig.11 Principal stress for the pipes in cohesive soil under different fault displacements

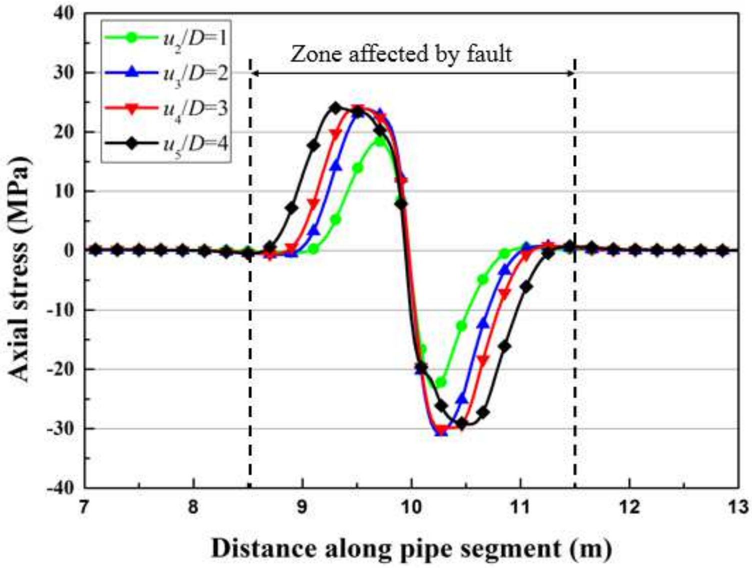

Fig.12 Axial stress of the buried PE80 pipes under different fault displacements

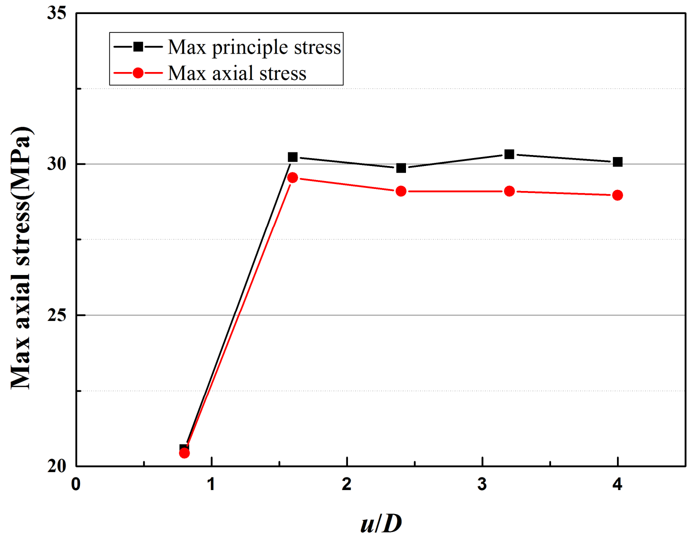

Fig.13 Max axial stress and max principle stress of the buried PE pipes

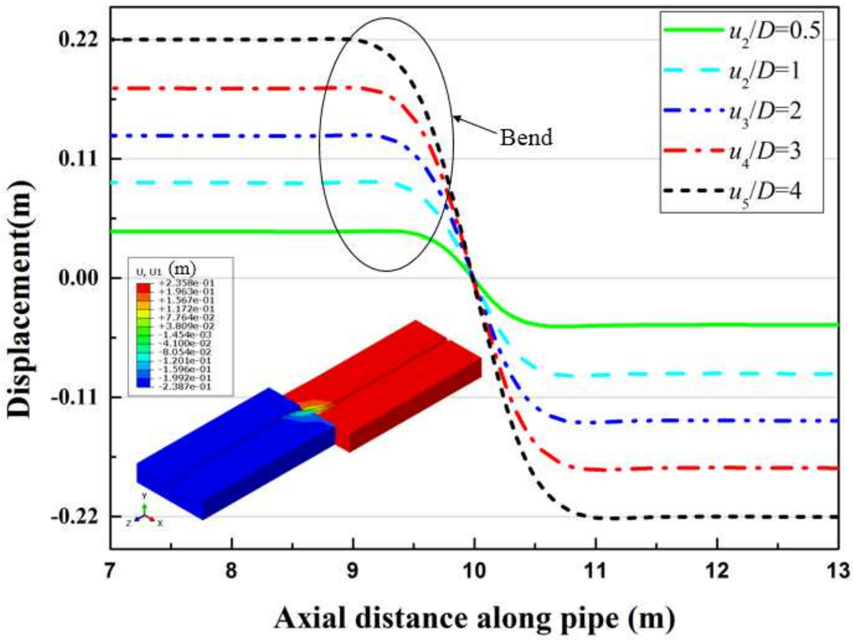

Fig.14 Deformation curves of non-pressure pipes under different dislocations

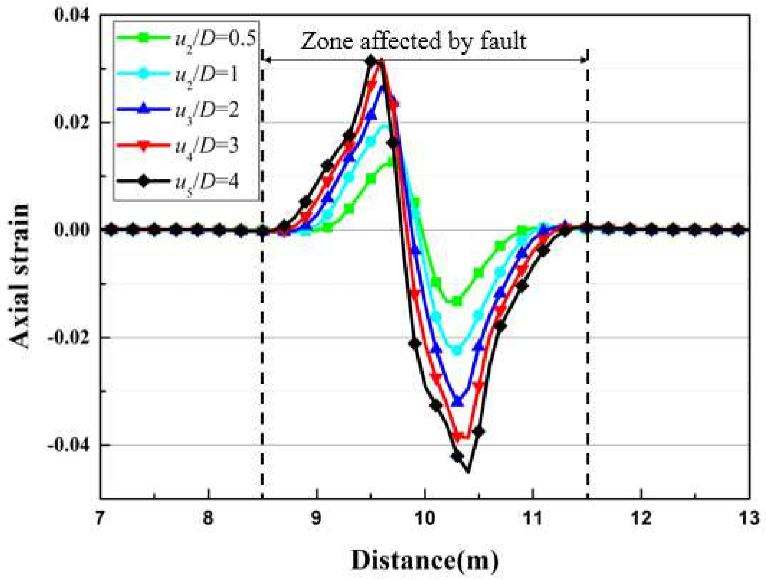

Fig.15 Axial strain of the buried PE pipes under different fault displacements

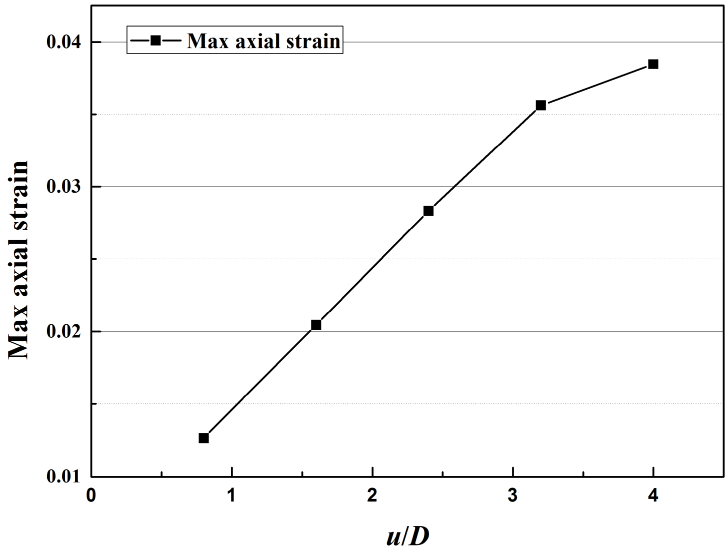

Fig.16 Max axial strain of PE pipes under different fault displacements

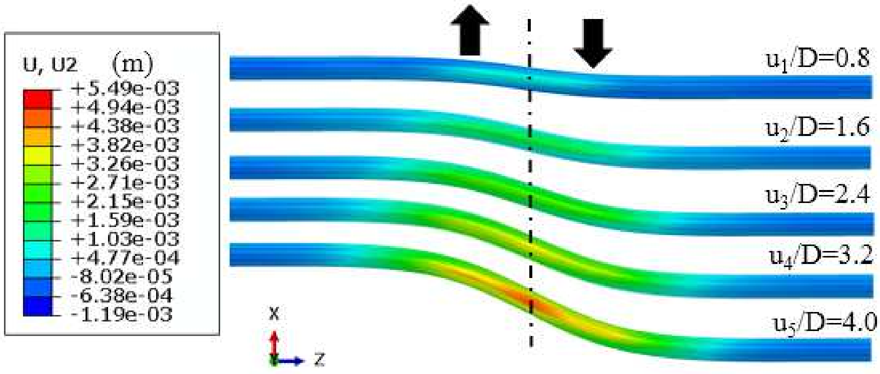

Fig.17 Displacement of PE pipes under different fault displacements

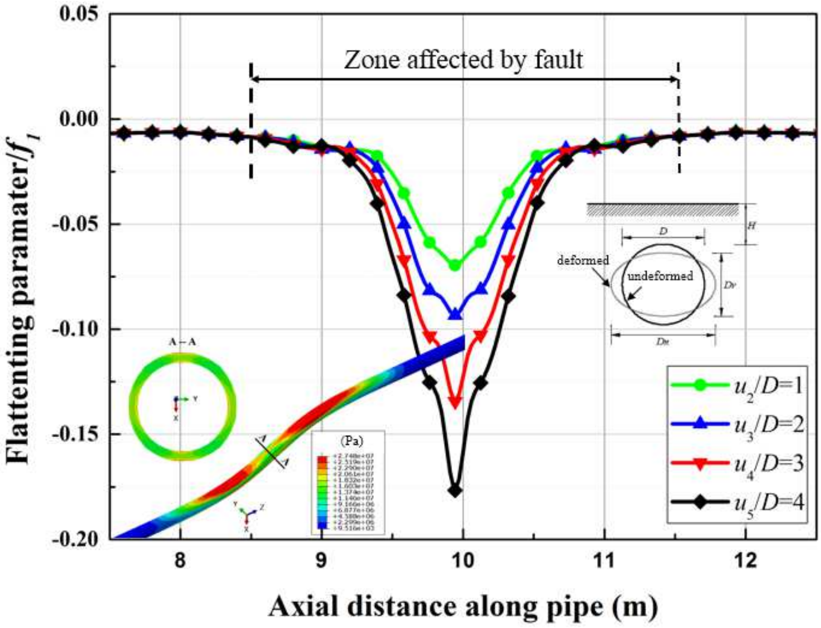

Fig.18 Flattening parameter f_1 along the non-pressure pipes under different fault displacements

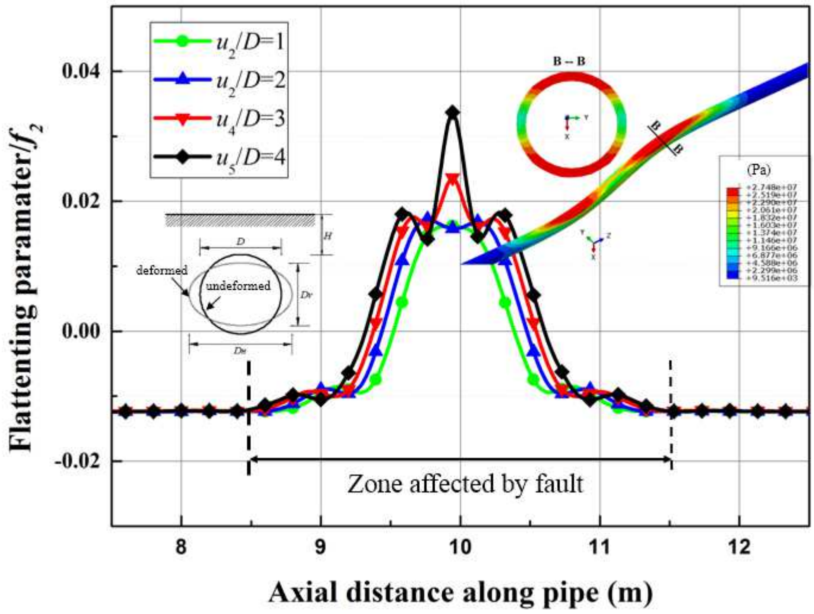

Fig.19 Flattening parameter f_2 along the non-pressure pipes under different fault displacements

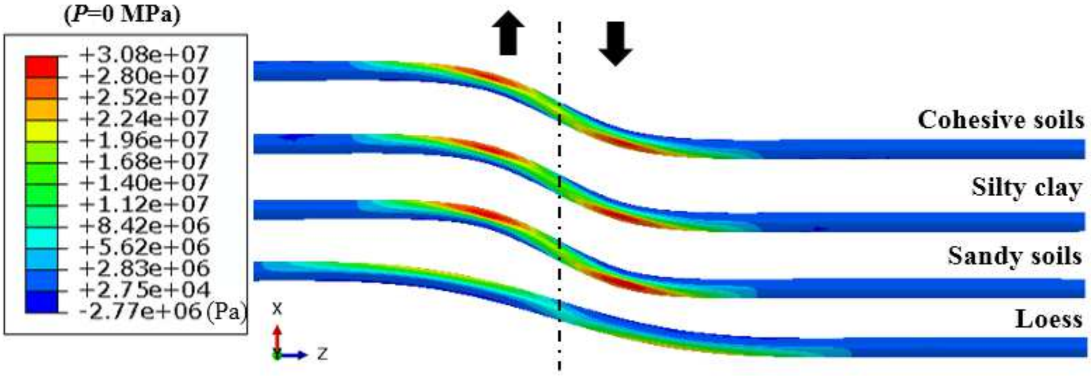

Fig.20 Principal stress of non-pressure pipes in different soils

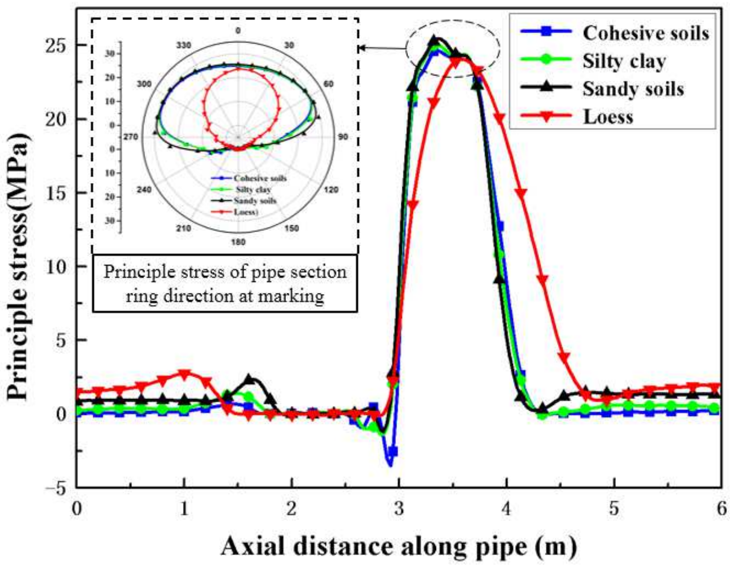

Fig.21 Principal stress along PE pipe segments in different soils

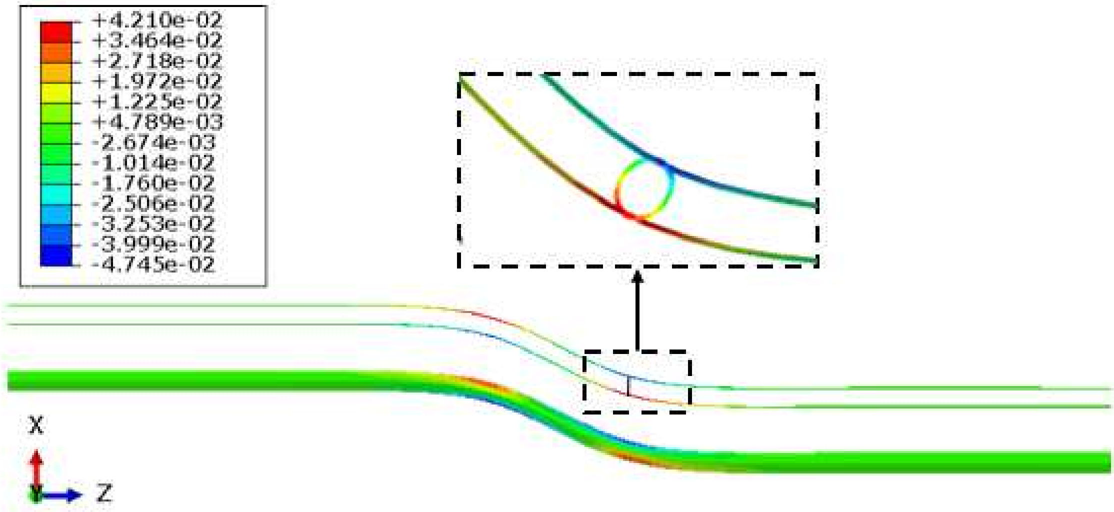

Fig.22 Axial strain of non-pressure pipes in silty clay

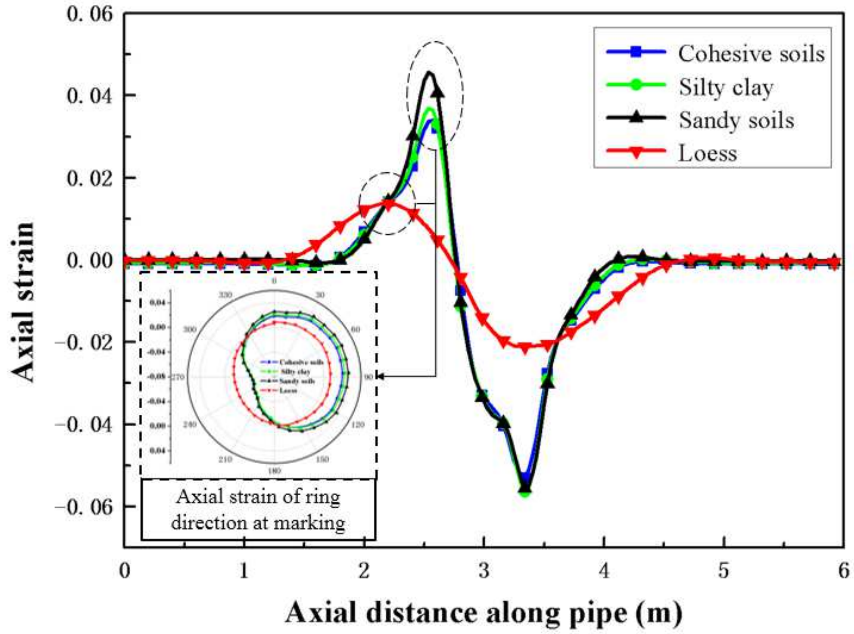

Fig.23 Axial strains along non-pressure PE pipe segments

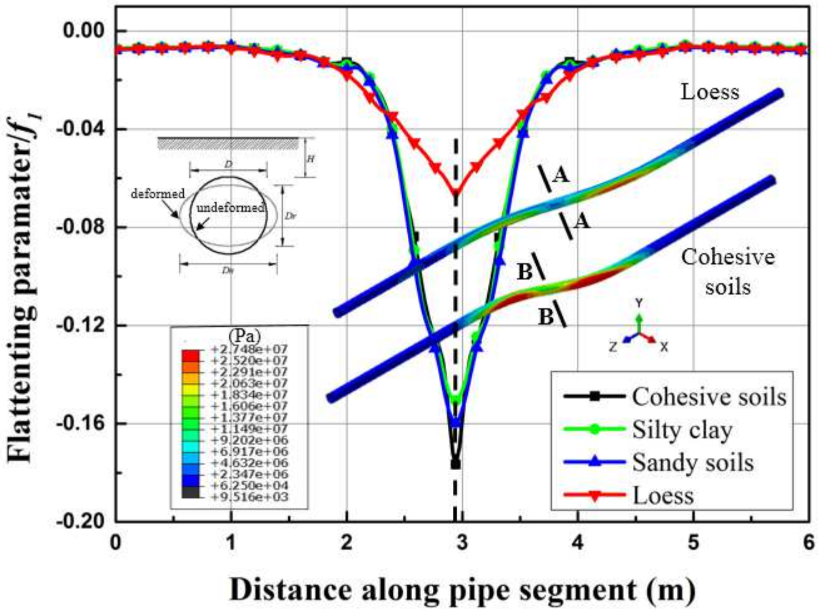

Fig.24 Flattening parameter f_1 along the non-pressure pipes in different soils

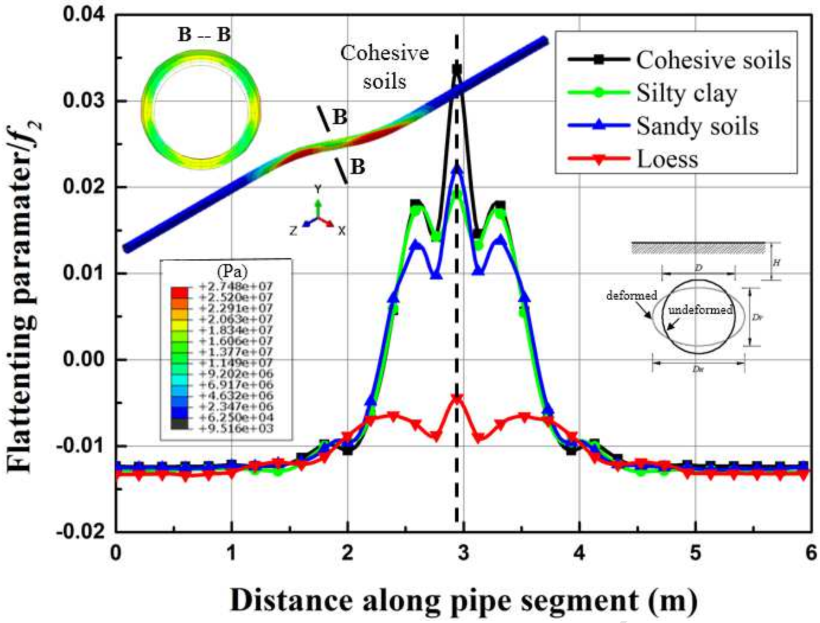

Fig.25 Flattening parameter f_2 along the non-pressure pipes in different soils

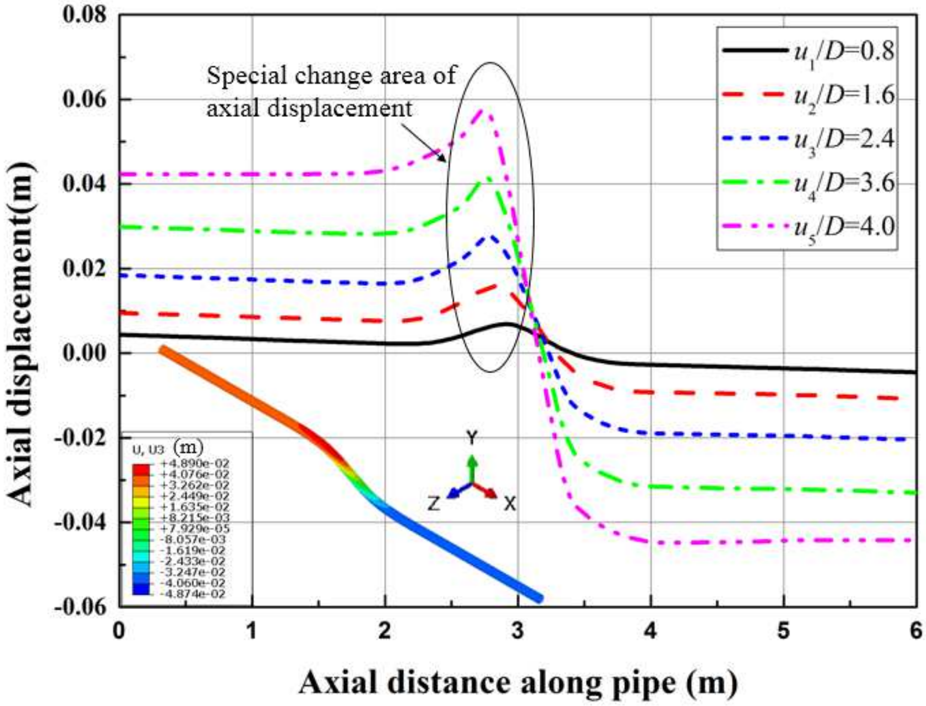

Fig.26 Displacement of pressurized PE pipe under different fault displacements

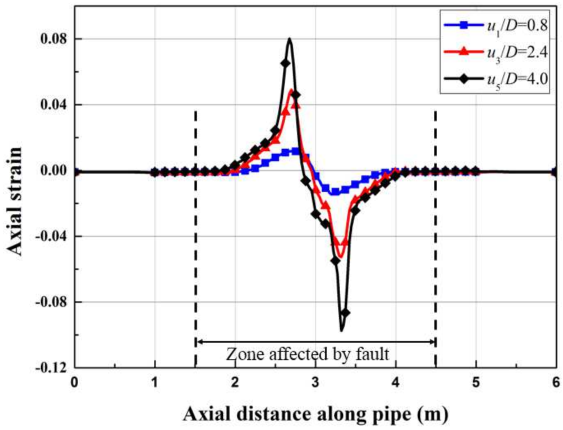

Fig.27 Axial strain of pressurized PE pipes under different fault displacements

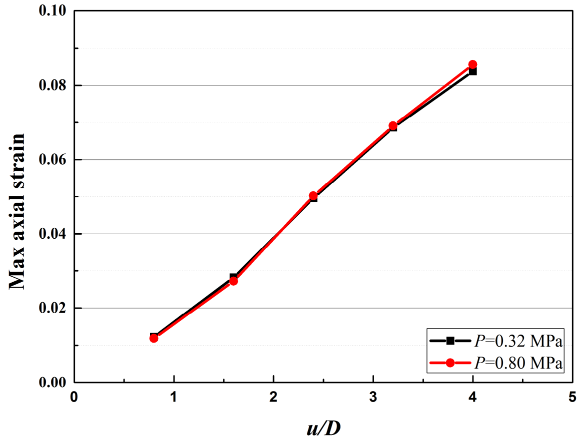

Fig.28 Max axial strain of pressurized PE pipes under different fault displacements

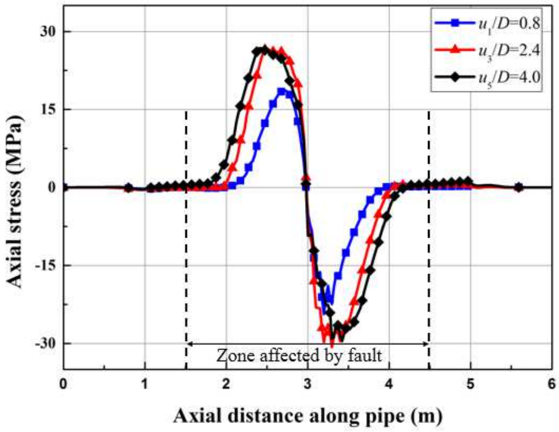

Fig.29 Axial stress of pressurized PE pipes under different fault displacements

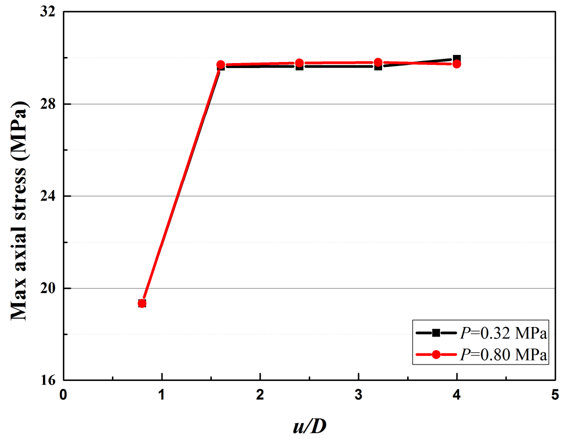

Fig.30 Max axial stress of pressurized PE pipes under different fault displacements

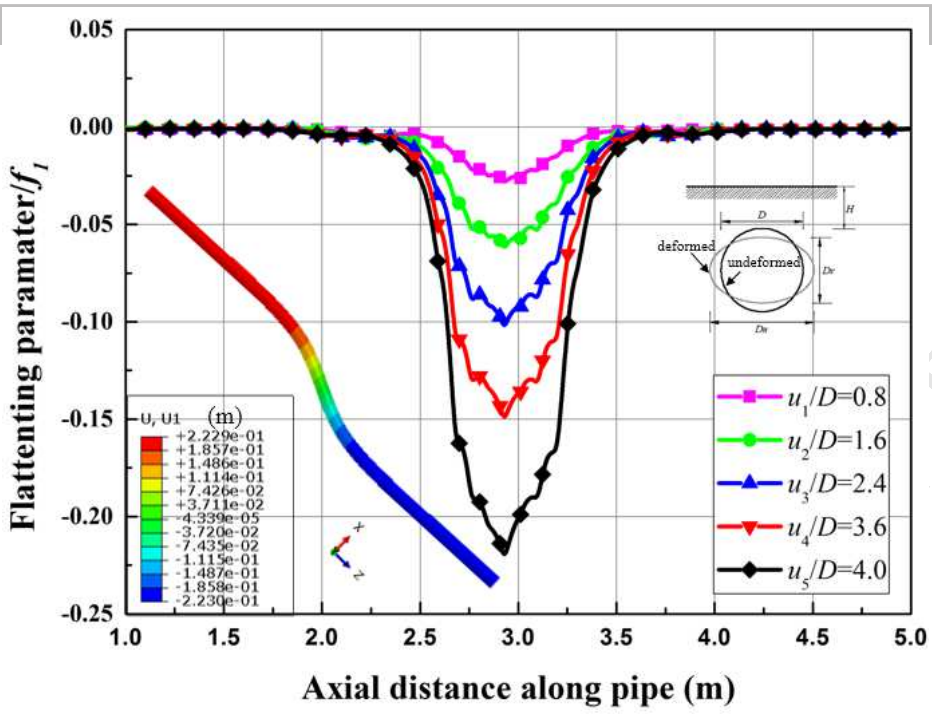

Fig.31 Flattening parameter f_1 along the pressured pipes under different fault displacements

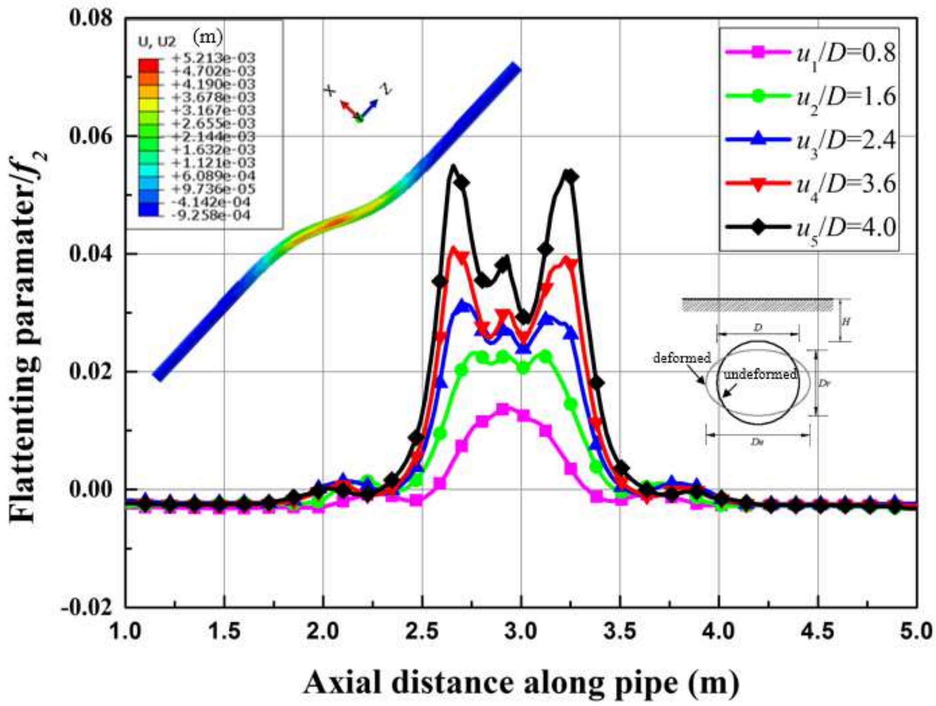

Fig.32 Flattening parameter f_2 along the pressured pipes under different fault displacements

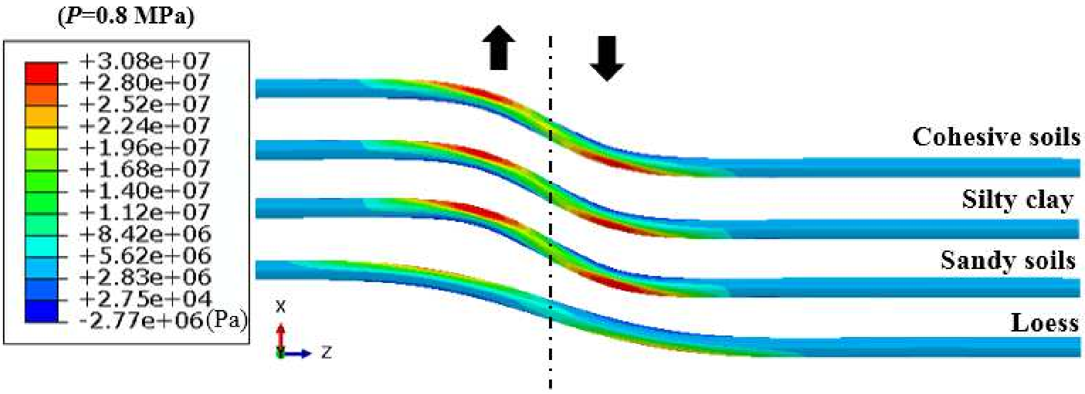

Fig.33 Principal stress of pressurized pipes in different soils

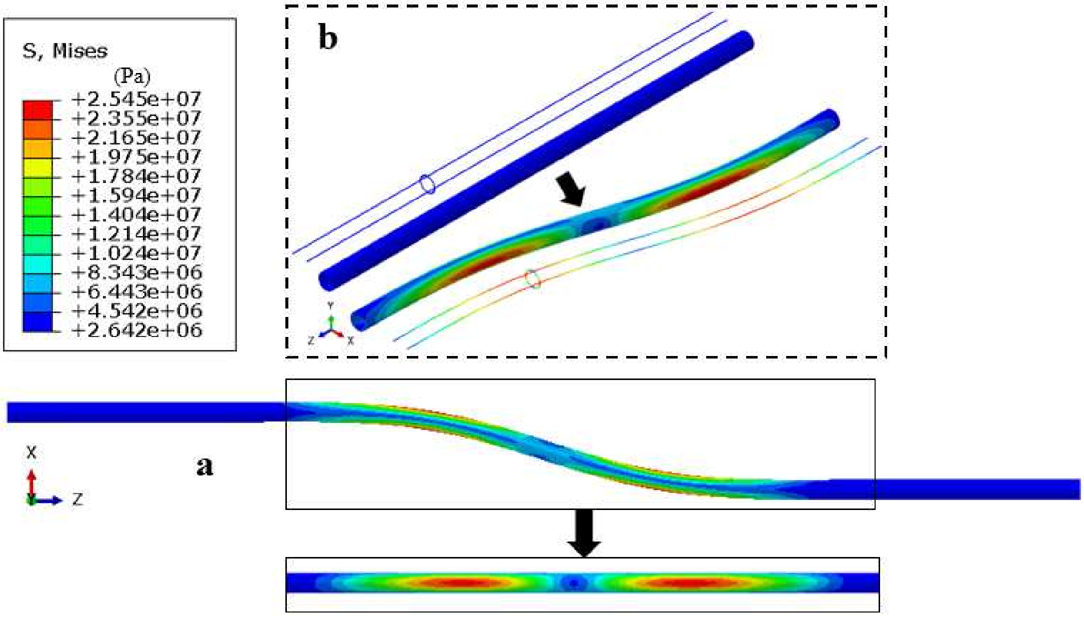

Fig.341 Stress distribution of pressurized PE pipe in loess. (a) different views and (b) selected axial and circumferential cross sections**.**

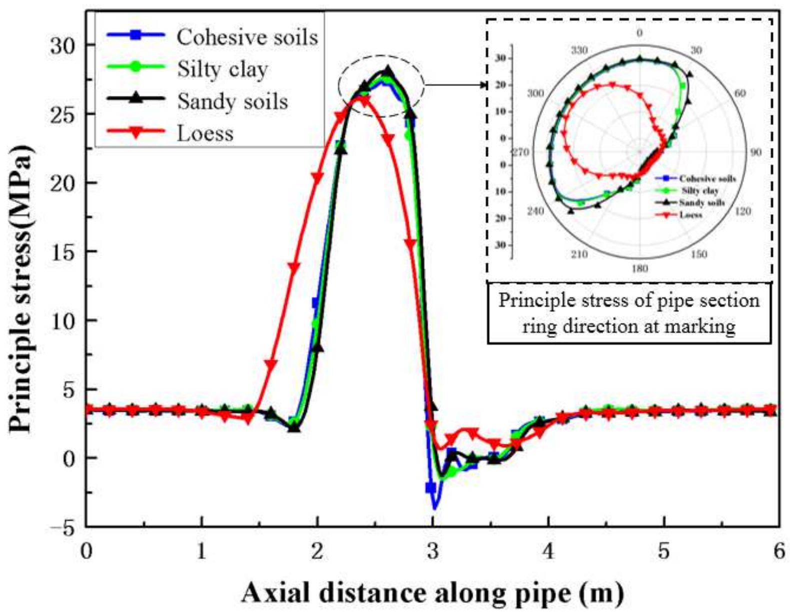

Fig.35 Principle stress along the pressurized PE pipe segments in different soils

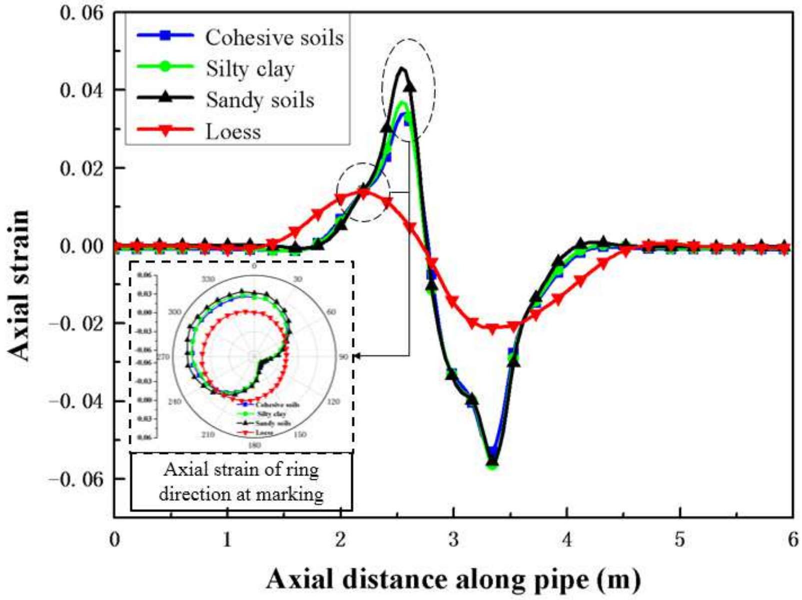

Fig.36 Axial strain along pressurized PE pipe segments in different soils

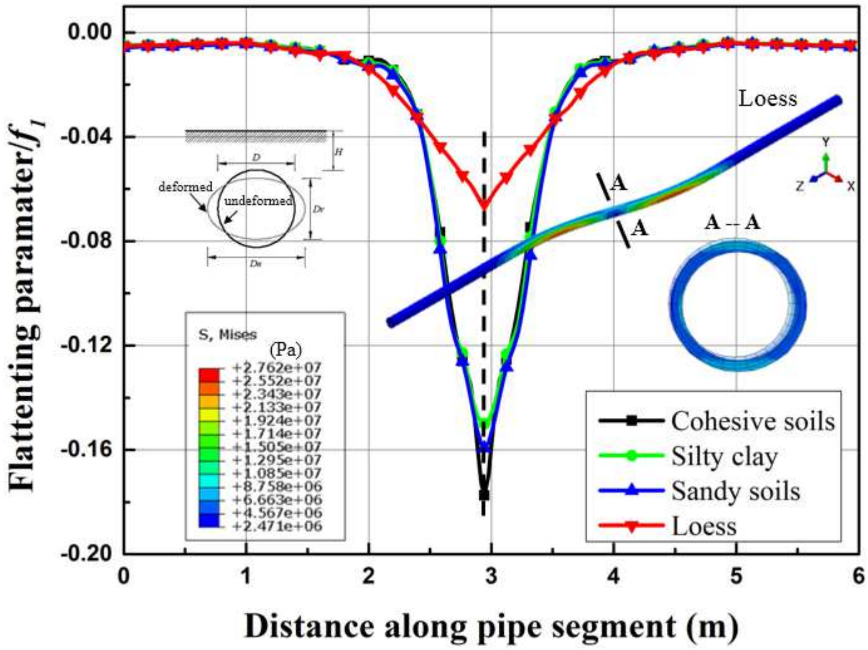

Fig.37 Flattening parameter f_1 along the pressured pipes in different soils

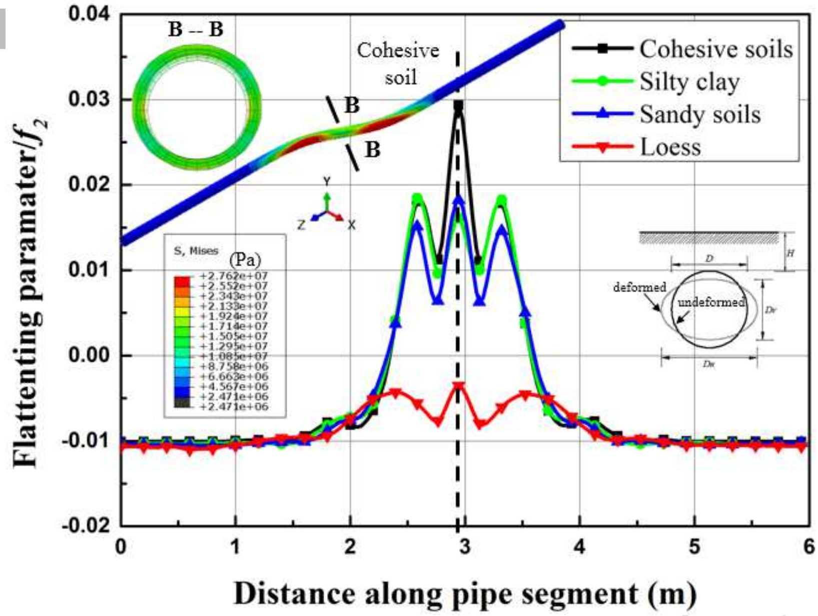

Fig.38 Flattening parameter f_2 along the pressurized pipes in different soils

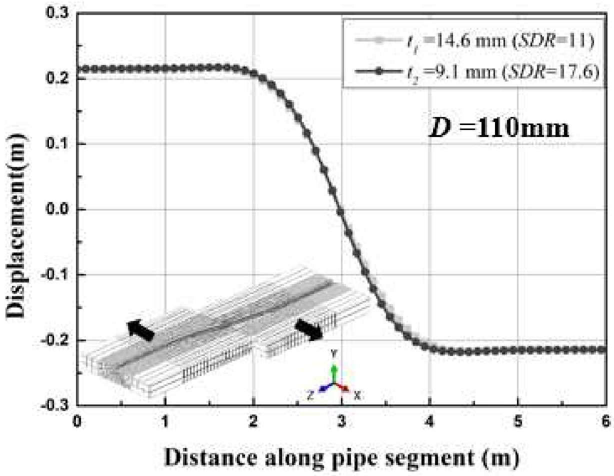

(a) The same *D*

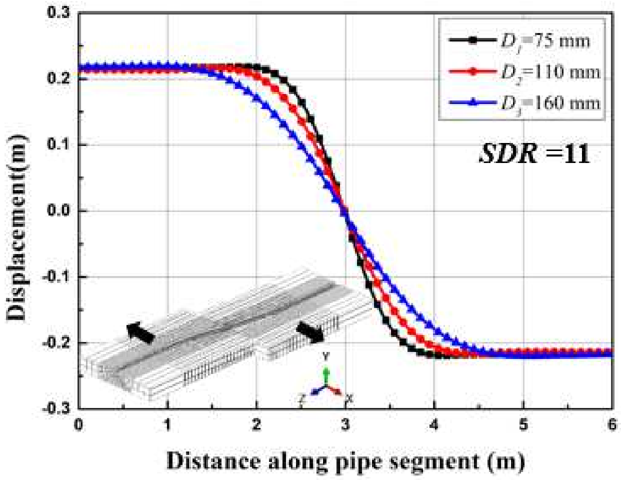

(b) The same *SDR*

Fig.39 Fault direction displacement of PE pipes with different sizes

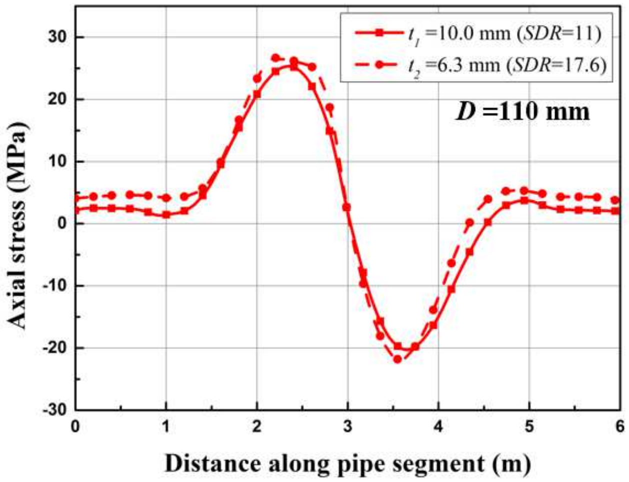

(a) The same D

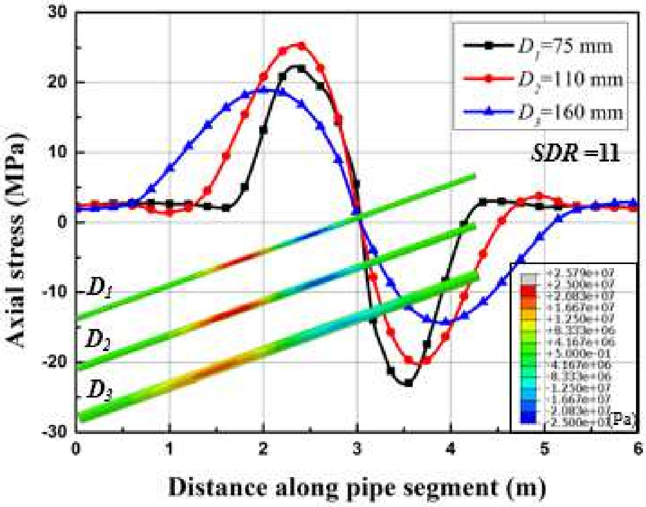

(b) The same SDR

Fig.40 Axial stress of PE pipes with different sizes

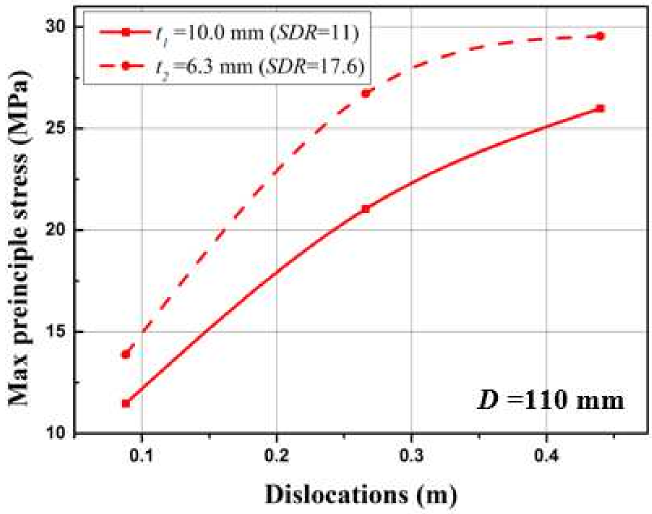

(a) The same *D*

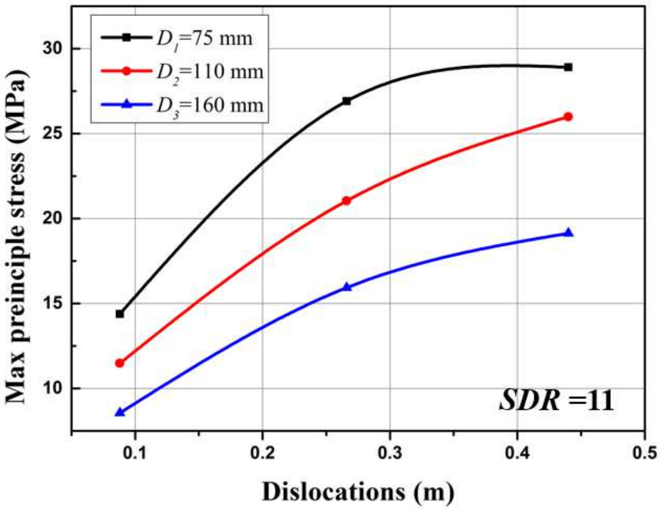

(b) The same *SDR*

Fig.41 Max principle stress of PE pipes with different sizes

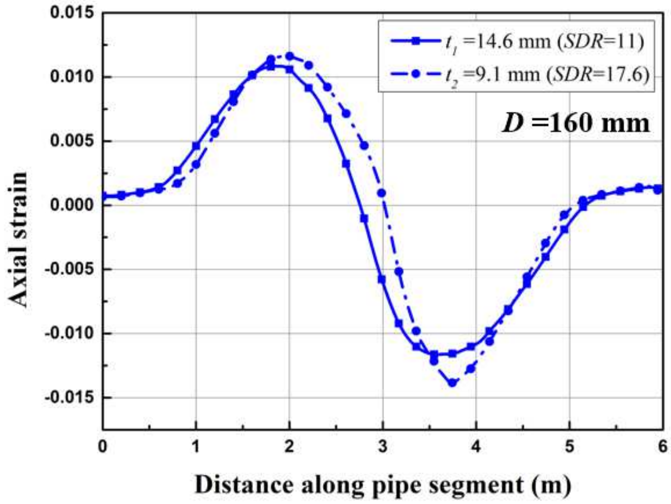

(a) The same D

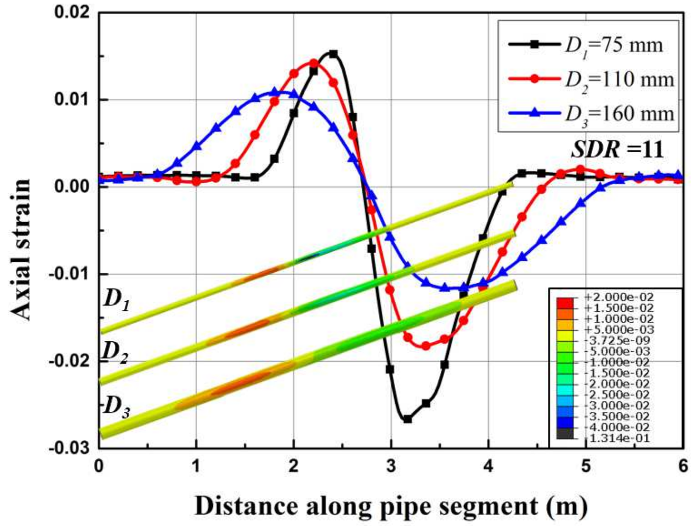

(b) The same SDR

Fig.42 Axial strain of PE pipes with different sizes

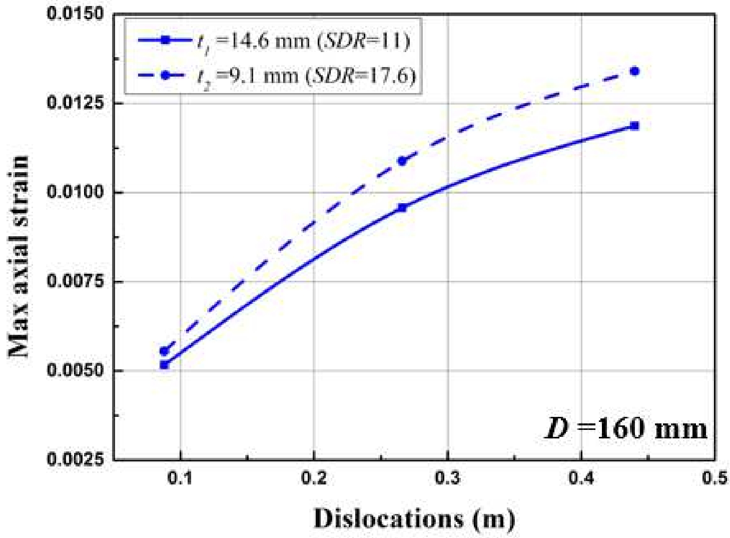

(a) The same *D*

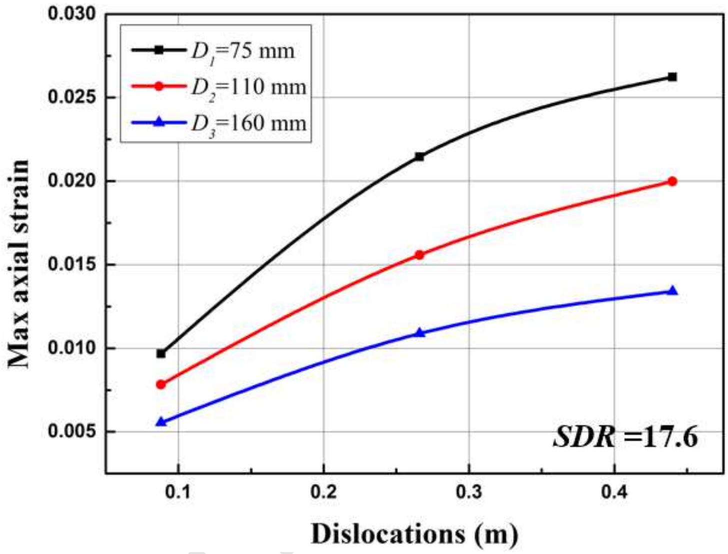

(b) The same *SDR*

Fig.43 Max axial strain of PE pipes with different sizes

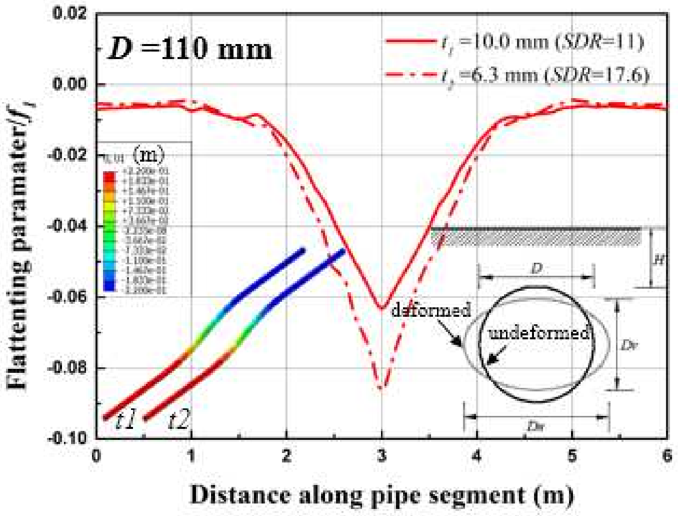

(a) The same *D*

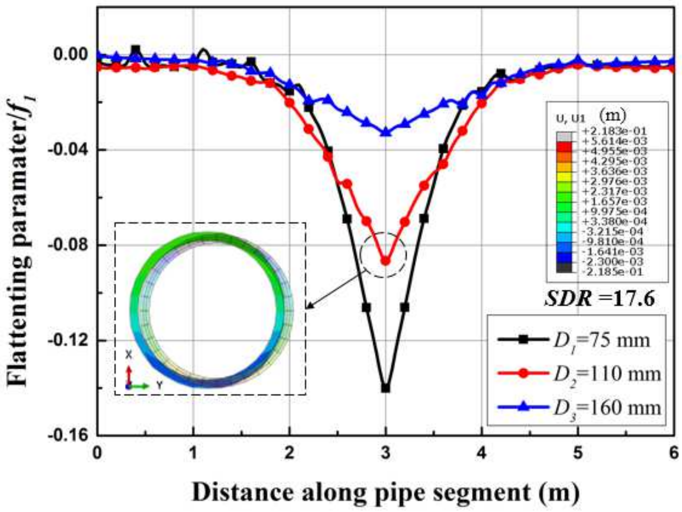

(b) The same *SDR*

Fig.44 Flattening parameter f_1 along the non-pressure pipe with different sizesd

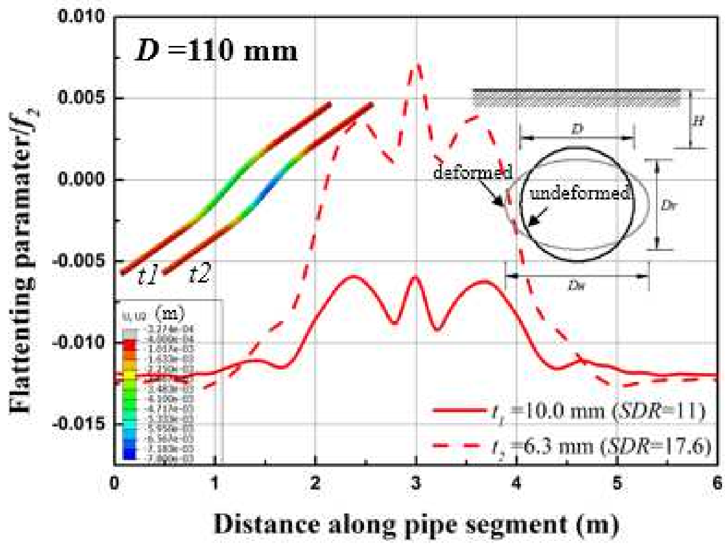

(a) The same *D*

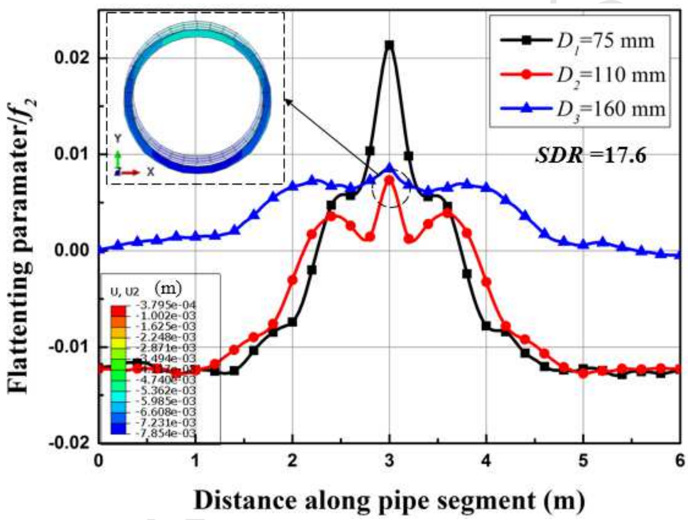

(b) The same *SDR*

Fig.45 Flattening parameter f_2 along the non-pressure pipe with different sizes

Highlights

Mechanical behaviors of PE pipes under strike-slip fault were investigated.

Effects of pressure, fault, soil and size on pipe's mechanical behavior were studied.

Gas pressure has less effect on the mechanical behavior of PE pipe.

Flatness curve of PE pipe is distributed symmetrically with respect to the fault plane.

Deformation rate of pipe increases with the increase of dislocation amount.